Aptamer-based detection of fumonisin B1: A systematic comparison with conventional and other novel methods

Vicente Antonio Mirón-Mérida[1,*], Yun Yun Gong[1], Francisco M. Goycoolea[1,*]

[1] School of Food Science and Nutrition, University of Leeds, Leeds LS2 9JT, UK; Y.Gong@leeds.ac.uk (Y.Y.G)
* Correspondence: fsvamm@leeds.ac.uk (V.A.M.M); F.M.Goycoolea@leeds.ac.uk (F.M.G.)

Abstract: Mycotoxin contamination is a current issue affecting several crops and processed products worldwide. Among the diverse mycotoxin group, fumonisin B1 (FB1) has become a relevant compound because of its adverse effects in the food chain. Conventional analytical methods previously proposed to quantify FB1 comprise LC-MS, HPLC-FLD and ELISA, while novel approaches integrate different sensing platforms and fluorescently labelled agents in combination with antibodies. Nevertheless, such methods could be expensive, time-consuming and require experience. Aptamers (ssDNA) are promising alternatives to overcome some of the drawbacks of conventional analytical methods, their high affinity through specific aptamer-target binding has been exploited in various designs attaining favorable limits of detection (LOD). So far, two aptamers specific to FB1 have been reported, and their modified and shortened sequences have been explored for a successful target quantification. In this critical review spanning the last eight years, we have conducted a systematic comparison based on principal component analysis of the aptamer-based techniques for FB1, compared with chromatographic, immunological and other analytical methods. We have also conducted an *in-silico* prediction of the folded structure of both aptamers under their reported conditions. The potential of aptasensors for the future development of highly sensitive FB1 testing methods is emphasized.

Keywords: Biosensors; mycotoxins; fumonisin B1; aptamers; aptasensors; analytical methods

1. Introduction

Mycotoxins are hazardous secondary metabolites produced by fungi, mainly *Alternaria*, *Aspergillus*, *Claviceps*, *Fusarium* and *Penicillium*. These biotic compounds act as hazards towards vertebrates, causing diseases when ingested, inhaled, or through skin contact. Some infectious processes, for instance, mycotoxicosis, take place after metabolization and accumulation of mycotoxins in several organs and tissues, due to immediate and progressive consumption of different contaminated food commodities [1], namely cereals, cocoa, coffee, fruit juices, milk and dairy, vegetable oils, beer, dried fruits, nuts, spices and their derived products. Multiple food matrices have been considered for the mitigation of toxin contamination [2], as mycotoxin occurrence takes place at different stages of the food chain, including field handling, storage and subsequent steps.

Exposure to mycotoxins is more likely to arise in regions with scarce methods for manipulation and storage of food products and can be related to other conditions such as malnutrition, limited regulations, and lack of protection for exposed groups [3]. Likewise, high-income countries are not exempt from mycotoxin occurrence, especially those importing agricultural and processed products from developing economies. As shown in Figure 1, there has been an increasing number of mycotoxin notifications in the last five years for the European Union (EU), whereas the United Kingdom (UK) has maintained a regular number of incidences, mostly identified through alerts, and border rejections of food and feed from EU member and non-member countries. To date, products such as peanuts, pistachios, hazelnuts, groundnuts, almonds, nutmeg, chilies, maize and dried figs are the most recurrent commodities exhibiting mycotoxin contamination; with a greater incidence in goods from Africa, South Asia, South America, China, USA and the Middle East [4].

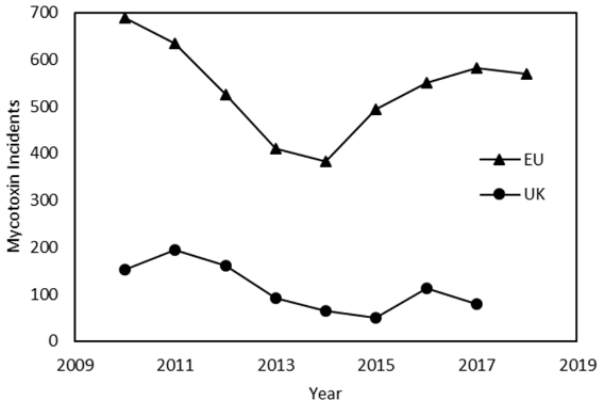

Figure 1. Number of mycotoxin notifications per year in the EU and the UK. Data based on the available Rapid Alert System for Food and Feed 2010-2018 by the European Commission [4] and the Incidents Annual Report 2010-2017 by the Food Standards Agency [184]

1.1 Fumonisin B1

Fumonisins are usually small alkyl amines containing two hydroxyl esterified propane tricarboxylic acids (tricarballylic acid), which are linked to adjacent carbons (Figure 2) [5]. When substituted in up to seven "R" side chains, the fumonisin aliphatic backbone serves as the basic structural unit for the conformation of different analogues. Existing fumonisin analogues can be classified in series A, B, C and P, where group B is the most abundant in nature [6]. Understanding the structure of fumonisins is critical when selecting and refining some quantification methods.

a)

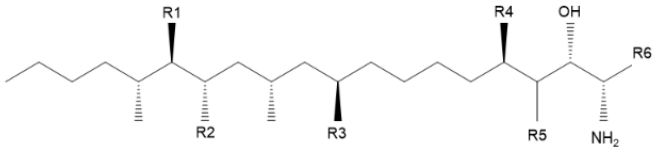

b)

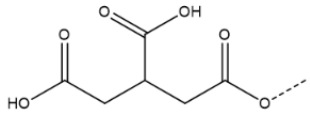

c)

Fumonisin	R1	R2	R3	R4	R5	R6
FB_1	TCA	TCA	OH	OH	H	CH_3
FB_2	TCA	TCA	H	OH	H	CH_3
FB_3	TCA	TCA	OH	H	H	CH_3
FB_4	TCA	TCA	H	H	H	CH_3
Iso- FB1	TCA	TCA	OH	H	OH	CH3
FBK1	=O	TCA	OH	OH	H	CH3
PHFB1a	TCA	OH	OH	OH	H	CH3
PHFB1b	OH	TCA	OH	OH	H	CH3
HFB1	OH	OH	OH	OH	H	CH3
FC1	TCA	TCA	OH	OH	H	H
FC3	TCA	TCA	OH	H	H	H
FC4	TCA	TCA	H	H	H	H
IsoFC1	TCA	TCA	OH	H	OH	H
OH- FC1	TCA	TCA	OH	OH	OH	H

Figure 2. Structure representation of (a)the general fumonisin backbone, (b)tricarballylic acid (TCA) and (c)a list of alkyl amine fumonisins (c) [6]

Fumonisins B1 and B2 were initially studied and isolated from Fusarium verticillioides, formerly known as *Fusarium monoliforme*. They were discovered during the investigation of compounds responsible for leukoencephalomalacia, toxicity and hepatocarcinogenicity in some animal species [6]. Early studies reported the main role of F. verticillioides in the production of FB1, FB2, FB3 (iso-FB2), FB4, FA1, FA2 and FC1 [7, 8, 9, 10], when cultivated in liquid cultures and solid matrices (maize). However, depending on the host crop and growth media, fumonisins can be generated by other fungal species such as *Alternaria alternata* on potato dextrose agar [11], stationary cultures of *Aspergillus niger* producing FB6 and FB2 [12, 13], and some strains of *Tolypocladium*

cylindrosporum, T. geodes and T. *inflatum* which developed fumonisins in high sugar media, when incubated at 25-30 ^{o}C [14].

1.2 Effects of fumonisin B1 on health

Classified as group 2B hazard, fumonisins B1 and B2, are possible carcinogenic to humans [15]. Fumonisin B1 causes multiple effects on different species, its toxicity was first related to the disruption of sphingolipid metabolism, as this mycotoxin inhibits ceramide synthase, which leads to both an increase in sphinganine and a decrease in complex sphingolipids, and further cell death observed in pig kidney cells [16, 17]. Notwithstanding this frequent assumption, studies on the protective role of liver X receptor (LXR) on FB1-caused hepatotoxicity implied the presence of different pathways [18].

Another mechanism triggered by FB1 is oxidative stress, where FB1 reduces mitochondrial and cellular respiration and increases the production of reactive oxygen species, as observed in rat astrocytes and human neuroblastoma cells [19]. In the same way, FB1 reduced growth of pig iliac endothelial cells and their barrier functions, while decreased the activities of some enzymes with antioxidant effects and enhanced the formation of lipid peroxidation compounds [20]. Exposure to fumonisin could also induce epigenetic changes such as DNA methylation and hypomethylation in rat glioma cells and human intestinal and hepatoma cells [19]. Apart from neurotoxicity, hepatotoxicity, nephrotoxicity, and carcinogenicity, FB1 has also been studied in corneal infections, due to its ability to form Langmuir monolayers on liquid surfaces [21]. Besides, some geographical studies have correlated the prevalence of esophageal cancer in humans with the presence of FB1 and FB2 in regional crops [22, 23].

In addition, adverse effects from fumonisins in human health were reported for Mexican American women living in the border region between Mexico and Texas, where fumonisin exposure was associated with neural tube defects [24]. Fumonisin B1 occurrence in Tanzania was reported in breastfeeding with contaminated milk as a current issue among children under six months of age [25]; elevated levels of dietary fumonisin were likewise related to inhibition of ceramide synthase in women from Guatemala [26], whose consumption of contaminated maize was detected in their high urinary fumonisin levels [27]. Other studies conducted in Tanzania have demonstrated the main role of fumonisin in underweight children due to breastfeeding and weaning within the first 36 months of age [28] as well as the high impact of substituting breastfeeding on the infant mycotoxin exposure [25]. Even though fumonisin B1 is not as prioritized as other mycotoxins, single exposure to it and its combination with other mycotoxins such as aflatoxins, represent an issue that needs to be addressed in deep, due to its common occurrence.

1.3 Fumonisin occurrence in food commodities and its worldwide regulation

The Food and Agriculture Organization (FAO) of the United Nations trough the worldwide regulations for mycotoxins in food and feed, indicated that by 2003 only 99 countries had regulations in place focused on mycotoxins. Additionally, the extent of those actions covered a brief group of different toxins among continents. As it can be noticed from Figure 3, the regulations for fumonisins in food and feed are established on either the sum of fumonisins type B1+B2+B3, B1+B2, or as total content of FB1 [29].

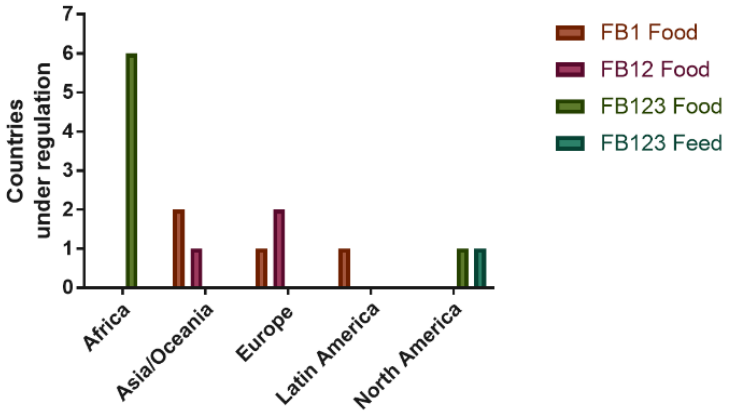

Figure 3. Countries regulating fumonisin in food and feed worldwide [29]

The number of countries under fumonisin regulations is equivalent for Europe and Asia/Oceania. On the other hand, the North America region has a noticeable approach by the United States, where limits for mycotoxins are targeted not only in food, but in feed. Based on the FAO controls, Africa was overall the less active region in enforcing mycotoxin regulations, particularly for any type of fumonisin. Paradoxically, though perhaps not surprising, the highest incidence of mycotoxins in food and feed occurs in Africa [30], however since 2011 a control for aflatoxin and fumonisin was established by the East African Community (EAS), whose scope included the six member countries, with a potential application on the trade activities by the twenty COMESA member states (Table 1). Furthermore, Latin America possesses a gap in recognizing fumonisins as an important group of hazardous compounds [29].

The growth of fumonisin producing fungal species has been reported on corn seedlings, grits, meal and flour, tomato leaves, seedlings and rice [5, 9, 31, 32, 33] as well as some dried samples comprising coffee beans and vine fruits [34, 35]. Some Fusarium species can produce fumonisins in media based on rice, oat, carrots and malt. In contrast, A. *niger* requires low water activity media and products with high sugar content [12, 35]. Maximum levels of fumonisins in both food and feed are shown in Table 1. As previously mentioned, cereals, rice and maize food and feed products are the most common targeted commodities for possible fumonisin outbreaks. Understanding the maximum values established by regulation, along with the expected contamination levels for distinct samples, is crucial during the design of conventional and novel quantification methods. Also, it is necessary to know the scope and applicability of each technique. The focus of this systematic comparison centers in these aspects by reflecting the state of the art in the field since 2012.

2. Methods

2.1 Systematic comparison

For this systematic comparison a screening was made from results obtained after searching the words “fumonisin + aptamer” and “FB1 + aptamer” in Scopus (28, 12), Web of science (28, 14), and Google Scholar (4, 32); as well as papers containing the specific DNA sequences. As indicated in Scheme 1, from the 29 relevant papers, 27 biosensors were identified and compared with other conventional methods for FB1 detection in terms of their limit of detection (LOD), assay time, and assay preparation time. The data were plotted in GraphPad Prism 7 to show the evolution and relation of such parameters throughout the years.

Table 1. Maximum permitted levels (µg/kg) of fumonisins in food and feed set by different organizations[1]

Commodity	Maximum Level (µg/kg)	Type	Authority	Regulatory Framework	Country
Raw maize grain	4 000	B1, B2	FAO, WHO	CODEX STAN 193-1995	International trade
Maize flour and maize meal	2 000	B1, B2	FAO, WHO	CODEX STAN 193-1995	International trade
Unprocessed maize (not for milling)	4 000	B1, B2	CEC	(EC) No 1126/2007	EU
Maize, maize-based foods for direct human consumption	1 000	B1, B2	CEC	(EC) No 1126/2007	EU
Maize-based breakfast cereals and snacks	800	B1, B2	CEC	(EC) No 1126/2007	EU
Processed maize-based foods and baby foods (Infants and young children)	200	B1, B2	CEC	(EC) No 1126/2007	EU
Milling fractions according to size (500 micron) and CN code 19041010	1 400 - 2 000	B1, B2	CEC	(EC) No 1126/2007	EU
Maize and processed products	1 000	B1, B2	MH	BG1	Bulgaria
Maize, rice	1 000	B1	MPH/INHA	CU1	Cuba
Cereals & cereal products	1 000	B1	DGCCRF	FR1	France
Maize	1 000	B1, B2	ISIRI, MOH	IR1	Iran
Corn & corn products	Not given	B1	SG1	AVA	Singapore
Maize	1 000	B1, B2	CH1	OFCACS	Switzerland
Maize products	According to the result of risk assessment	B1	-	-	Taiwan
Degermed dry milled corn products (e.g. flaking grits, corn grits, corn meal, corn flour with fat content of <2.25%, dry weight basis)	2 000	B1, B2, B3	US4, US5	FDA	USA
Cleaned corn intended for popcorn	3 000	B1, B2, B3	US4, US5	FDA	USA
Whole of partially degermed dry milled corn products (e.g. flaking grits, corn grits, corn meal, corn flour with fat content of ≥2.25%, dry weight basis); dry milled corn bran; cleaned corn intended for masa production	4 000	B1, B2, B3	US4, US5	FDA	USA
Corn and corn by-products intended for equids and rabbits	5 000	B1, B2, B3	US4, US5	FDA	USA
Corn and corn by-products intended for swine and catfish	20 000	B1, B2, B3	US4, US5	FDA	USA
Corn and corn by-products intended for breeding ruminants, breeding poultry and breeding mink (includes lactating dairy cattle and hens laying eggs for human consumption)	30 000	B1, B2, B3	US4, US5	FDA	USA
Ruminants ≥ 3 months old being raised for slaughter and mink being raised for pelt production	60 000	B1, B2, B3	US4, US5	FDA	USA
Poultry being raised for slaughter	100 000	B1, B2, B3	US4, US5	FDA	USA
All other species or classes of livestock and pet animals	10 000	B1, B2, B3	US4, US5	FDA	USA
Maize grains/ Millet flour	2 000	Fumonisin	EAC	EAS	Burundi, Kenya, Rwanda, South Sudan, Tanzania, Uganda.

[1] Abbreviations: **AVA:** Agri-Food and Veterinary Authority; **BG1:** Ministry of Health in coordination with the Ministry of Agriculture and Forestry, the Ministry of Industry and the State Standardization Agency (2000). Regulation No.11/2000 of 11 July 2000 laying down the maximum levels of mycotoxins in foodstuffs. Official Newspaper of the Republic of Bulgaria No. 58: 18-24.; **CEC:** Commission of the European Communities; **CH1:** Verordnuung uber Fremd-und Inhaltsstoffe in Lebensmitteln. SR817.021.23; **CN:** Combined nomenclature; **CU1:** Ministerio de Salud Pública (1999). Manual de indicadores empleados en la evaluación sanitaria de alimentos. Instituto de Nutrición e Higiene de los Alimentos (INHA), Diciembre de 1999; **DGCCRF:** Direction Generale de la Concurrence, de la Consommation de la Repression des Fraudes, Ministere de l'Economie, des Finances et de l'Industrie; **EAC:** East African Community, **EAS:** East African Standard 89: 2011, ICS 67.060; **EC:** Commission Regulations**; FAO:** Food and Agriculture Organization of the United Nations: **FDA:** Food and Drug Administration; **FR1:** Avis du Conseil Superieur d'Hygiene Publique de France du 8/12/1998; **IR1:** National standard of Institute of Standard and Industrial Research of the Islamic Republic of Iran (ISIRI) [2002]. Maximum tolerated levels of mycotoxins in food and feeds. No.5925; **ISIRI:** Institute of Standard and Industrial Research of the Islamic Republic of Iran; **MH:** Ministry of health; **MOH:** Ministry of Health and Medical Education; **MPH/INHA:** Ministry of Public Health/Instituto de Nutrición e Higiene de los Alimentos; **OFCACS:** Official Food Control Authorities of the Cantons of Switzerland; **SG1:** Regulation 34 of the Singapore Food Regulations; **US4:** FDA (2001). Guidance for industry: Fumonisin Levels in Human Foods and Animal Feeds, November 9, 200; **US5:** FDA; **WHO:** World Health Organization

2.2 Principal component analysis

The aptamer-based biosensors for FB1 detection and several conventional and novel methods published since 2012 (publication year of the first aptasensor), were combined in a principal component analysis, performed in Minitab 15 Statistical Software. Before the application of the correlation matrix, all data were treated according to the following equations:

$$LODt = \frac{LOD\ max}{LOD} \qquad ATt = \frac{AT\ max}{AT} \qquad APt = \frac{AP\ max}{AP}$$

Where LODt , ATt and APt are the treated limit of detection, assay time and assay preparation time, respectively; LODmax and ATmax are the maximum limit of detection and maximum assay time for all the data in this comparison (since 2012), equal to 3200 µg/L [90] and 720 min [166] respectively. The assay preparation time was calculated by adding the reported times for sample extraction,

synthesis of nanoparticles, support treatment, and array assembling. The maximum preparation time per assay was calculated as 12900 min [151]. This mathematical treatment allowed to determine the correlation of the maximum values to the most sensitive, fast and therefore, effective methods.

2.3 DNA folding

The DNA folding forms of the four existing aptamers were predicted with mfold Web Server according to their reported folding conditions.

3 Conventional and novel methods for mycotoxin identification

Typical methods for the identification of mycotoxins in food samples incorporate compound separation principles for quantification through TLC, HPLC, and LC-MS. At the same time, some commercial immunoassays optimized the use of antibodies for mycotoxin quantification. However, most of them utilize expensive and sophisticated equipment for time-consuming assays that are required to be performed by skilled operators, as they utilize complex elements and instruments [36, 37]. Novel approaches including optical, electromagnetic, electrochemical and surface-sensitive techniques (e.g., surface plasmon resonance, ion-selective field-effect transistors, surfaced-enhanced Raman spectroscopy) along with aptamer-based techniques, have been developed and found to exhibit comparable and even higher sensitivities in than that of conventional procedures.

Based on Tables 2-5, the LODs of different reported methods were plotted against their total assay times, as reflected on Figure 4a. The assay time was calculated from either the divulged times at either the injection step in chromatography, or the incubation between the antibody/aptamer/recognition region with its corresponding target molecule. This consideration excluded any pre-treatment, extraction steps and particle fabrication, as those phases were part of the assay preparation time (Fig 4b). The shortest response time for the analysis of extracted samples was achieved in seconds to minutes, when using Surface-enhanced Raman spectroscopy [140]. Nevertheless, some sensors qualified as fast required overnight steps and long incubation times for the whole system arrangement, especially when the synthesis of nanoparticles and drying phases were required. Assay times below ten minutes were achieved through chromatographic, immunoassays, and some innovative methods, nonetheless the more sensitive assays were secured with aptamer-based biosensors [170, 177, 200], immunosensors with carbon nanotubes [101, 109], and molecularly imprinted polymer nanoparticles (MIPs) [191], as indicated in Figures 4a and 4c.

In addition to high specificity, the combination of minimum assay times with low limit of detections is ideal for an appropriate quantification technique. Nonetheless, an increase in the assay preparation time can complicate the achievement of on-site/point of care analysis and compromise the reproducibility. Even though there is high sensitivity achieved through aptasensors, such DNA-based techniques along with some immunoassays, entail long assay times with extended preparation time, due to incubation and platform preparation, respectively (Figure 4b). In those cases, the final response was normally measured as either a fluorescent or a colorimetric signal. Figure 4c portrays the LODs accomplished per year, where it can be noted that ongoing research is still focused on developing chromatographic techniques and immunoassays.

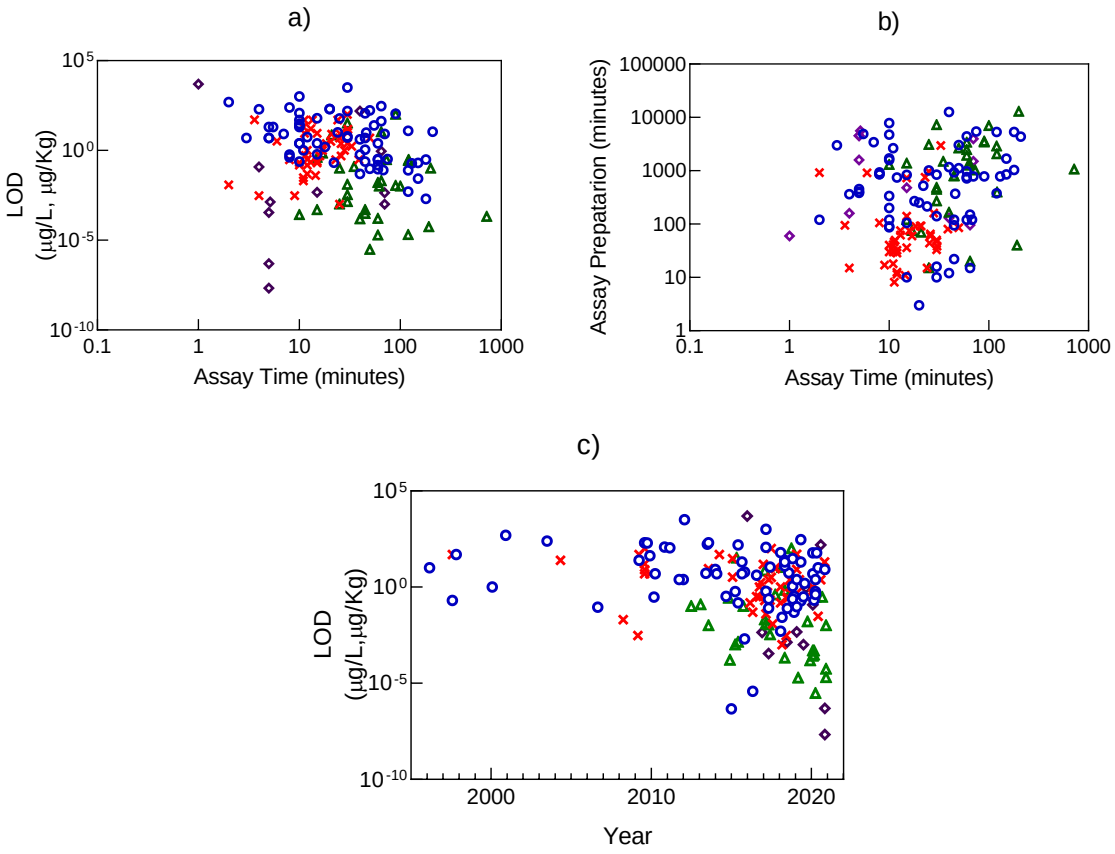

Figure 4. Relation of the assay time with (a) the limit of detection (LOD) and (b) assay preparation time for the approaches reported since 2012, (c) and LODs achieved over time through different methods (**O**: Immunologic, **X**:Chromatographic, **Δ**: Aptamer-based, **◊**: Other)

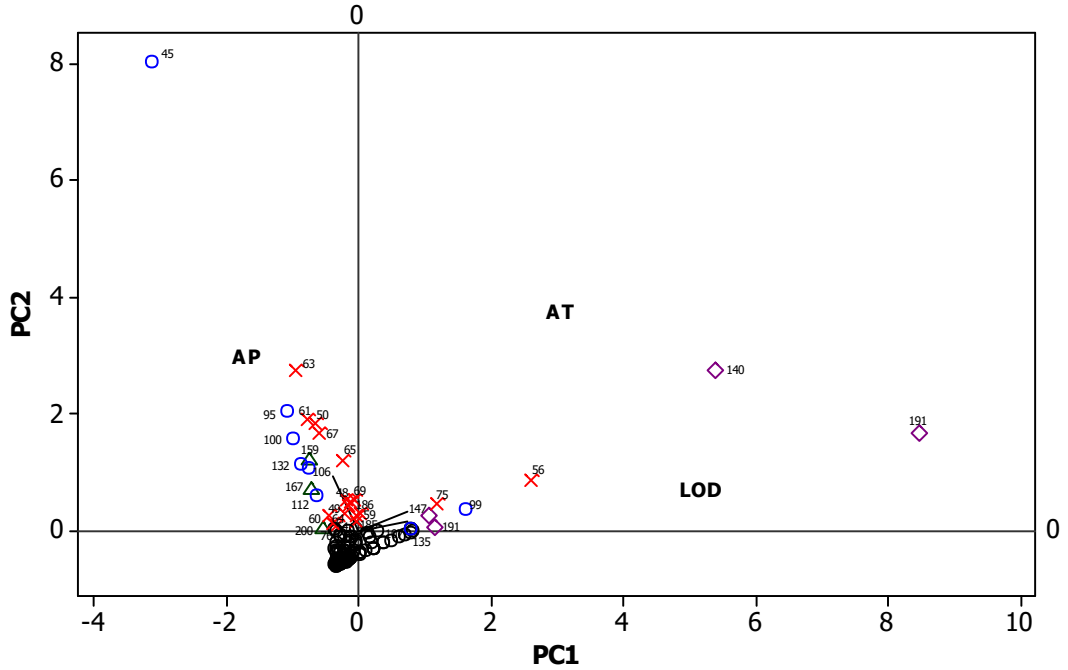

Figure 5. Principle component analysis for the correlation of aptasensors and conventional methods reported from 2012 to the lowest detection limits (LOD), assay time (AT) and assay preparation time (AP). (**O**: Immunologic, **X**: Chromatographic, **Δ**: Aptamer, **◊**: Other). The numbers correspond to the correlated references from Tables 2-5.

Although, over the last five years there has been an improvement on the detection limits of some protocols, especially for immunoassays whose LODs have reached the picogram scale, most of the new chromatographic and antibody-based methods still quantify values comparable to earlier findings. Conventional assays with the highest sensitivity have included electrochemical designs, electrochemiluminescent quantifications, and MS detection (Table 2-3). Of note, fluorescent, colorimetric and electrochemical aptamer-based sensors reported over the last three years, accomplished relevant LODs with a promising tendency (Figure 4).

Despite the fact that the use of antibodies with electrochemical readouts was advantageous for achieving some of the lowest LODs for fumonisin B1, equivalent to 4.6e-7 and 3.7e-6 µg/L [101, 109], these immunosensors were not included in the principal component analysis (PCA), as no assay time was reported in either case. Hence, as indicated in Figure 5, LC-MS [56,75], immunoassays with optical [99,107,135], Raman (due to its quick procedure) [140], fluorescent readouts [147] and electrochemical MIPs [191] were correlated to the combination of low LODs with short assay times. However, such statistical analysis did not show the advantages of aptamer-based methods, which was also observed on the correlation of short assay preparation times with LC-MS, immunologic and only three aptasensors [159, 167, 200]. This was shown by PCA, where the main drawbacks from aptamer-based sensors for FB1 was their long assay and assay preparation times denoted by is absence of correlation in both components when compared to other methods.

3.1 Chromatographic detection of fumonisin B1

Together with immunoassays, chromatographic methods for the quantification of mycotoxins, have been widely studied and optimized for the analysis of several food products as indicated in Table 2. Initial chromatographic techniques were focused on the exclusive quantification of fumonisin in corn, through the analysis of either MS/MS or fluorescence signals. Following analysis confirmed the good correlation of maize-based products expenditure with FB1 levels in human urine [40]; which consolidated its utilization as a relevant biomarker, as a portion of ingested FB1 is excreted in urine [44].

The detection of fumonisins is limited by its absence of fluorescence; therefore, the introduction of a chromophore for the derivatization of the amino groups within fumonisin is always required [179]. Initial derivatization procedures utilized maleic anhydride derivatives and fluorescamine [7,180]. Nevertheless, more sensitive detection procedures introduced but still utilize pre-column derivatization with o-phthaldialdehyde [39, 42, 46, 181, 182], naphthalene-2,3-dicarboxaldehyde [41], and the quick and stable (9-fluorenylmethyl) chloroformate (FMOC) [55,183].

Fluorescence detectors are restricted for the individual quantification of FB1 [38, 46, 47], the sum of FB1, FB2, FB3 [41] or the separate determination of up to three group B fumonisins [42, 55]. On the other hand, one of the main advantages of mass spectrometry detectors is the possibility of performing multiplex analysis, not only for different mycotoxins [48, 49, 50, 53, 54, 57, 58, 59, 60, 61, 64, 65, 66, 67, 71, 72, 73, 74, 77, 79, 80, 187], but also when combined with varied metabolites. Growth regulators, antibiotics, pesticides [51, 70, 75], and other fungal metabolites [63, 68], were simultaneously identified in analysis capable of assessing up to 74 and 90 compounds [62,78]. Mass spectrometry has also been used for assessing mycotoxin transfer from feed to organs and tissue in poultry [80]

The importance of novel analytical methods relies on the low sensitivities achieved within a relatively short detection time. The speed of mass spectrometry (ESI+) signals, was early proven to reduce the sole determination of FB1 in bovine milk to 4 minutes [43], with a half-fold time reduction on more recent assays for pig samples (plasma, urine, feces) [56]. Its limits of detection have reached 0.003 µg/kg [43, 65] for animal (pig) and food samples (corn meal), and 0.001 µg/L in human urine [73]. Notwithstanding the excellent performance of conventional analytical methods, some disadvantages are related to sample pre-treatment including long extraction steps with further purification protocols, as well as method optimization of the chromatographic separation, derivatization or internal standard addition, along with its corresponding validation method. For instance, a single drying step could add two days to the total assay preparation time [53].

Sample clean-up is a key step for reducing matrix effect, where strong anion exchange (SAX) columns have been utilized as cheaper clean up cartridges in LC-MS detection, with recoveries of up

to 86.6 and 106% for human hair [47] and piglet urine [56] respectively. In a similar way, immunoaffinity columns (IAC) have been proven to attain maximum recoveries of 109% for FMOC-derivatized cornmeal samples [55], and 90% in rice analyzed by LC-MS [75]. The specificity of antibodies in IAC also allowed the successful LC-MS analysis of FB1 in complex samples, such as milk [43], human urine [44] and chicken tissue [80] with peak recoveries of 88.4%, 99.1% and 95-102% respectively. Lower recoveries were found for the determination of OPA-derivatized FB1 in maize (68.5%), rice (72.4%), sorghum (75.6%) and wheat (69.4%) extracts [42]. Nonetheless, IACs increase the total assay cost, since they could account for double or triple the price of SAX cartridges, with highly comparable performance. Besides, IACs have a limitation on the variability of analytes and could promote interaction with the matrix constituents [77]. In both cases (SAX and IAC) the total analysis time is enlarged by the conditioning, loading, washing, elution, evaporation, and reconstitution steps.

Some novel developments incorporated magnetic nanoparticles for the sorption and concentration of mycotoxins, promoting a simultaneous clean-up and sensitivity enhancement in the overall method [59]. Nonetheless, even when the performance of patented commercial clean up columns allows their utilization in single [39] and multiple mycotoxin analysis, the adsorption procedure of recent products might impede the detection of FB1 and FB2 [53]. As a replacement, novel dispersants such as nano zirconia, have been found with high extraction efficiency of FB1 [65].

Alternatively, the QuEChERS method, initially developed for pesticides, was subsequently introduced for the dispersive solid-phase extraction (SPE) of FB1 [46], and further validated for its application in the multi-target analysis due to its lower cost, less time consumption, easy procedure [50, 52, 63, 185, 186], as well as its availability in extraction kits [54] with satisfactory recoveries [60]. Likewise, sample preparation with a QuEChERS dispersive SPE was useful for minimization of matrix effects from beer, with a preconcentration step producing enhanced LODs [74]. In spite of being a favorable option for sugar reduction in the quantification of FB1 in oat, soy and rice beverages (extraction recoveries 80, 82, 85%; matrix effect: 76, 63, 75%) [61], a UPLC-MS/MS study of *Alpinia oxyphylla* revealed the unsatisfactory FB1 and FB2 recoveries from QuEChERS (~50 & 55%) and hydrophilic-lipophilic balance (HLB) cartridges (~65 & 55%) in comparison to solid-liquid extraction (~80 & 70%). Nevertheless, the three extraction methods exhibited a signal increase (80-145%) due to matrix effect [64]. By contrast, recent studies in sugarcane juice proposed the use of HLB cartridges as an alternative to QuEChERS, due to its high recoveries of 98% for FB1 [79].

Despite the expected disadvantages of the dilute and shoot method towards the complexity of some samples, which could affect the detector sensitivity and assay performance, when optimized, this procedure can be applied in the multi-target analysis of food samples without a clean-up phase [61, 68, 70, 75]. For instance, a comparison between the efficiency of dilute and IAC methods revealed that, even when lower LODs and limits of quantification (LOQs) were obtained with the clean-up step (0.5 and 1.66 against 2.3 and 4.3 µg/kg), a dilution procedure accomplished improved regression (0.9941), high recoveries (94-106%) and reproducibility for FB1-spiked animal feed [77].

A similar situation was confirmed for matrix-match calibration [45, 49, 70], and internal standard (IS) addition [48, 66, 77] where a clean-up step was not necessary to eliminate matrix effects and run accurate determinations. Yet, the use of specific IS and a validated method for a single matrix, could reduce the scope of the determination, and increase its final cost. Notwithstanding, some approaches proposed the application of the aforementioned procedures combined with clean up techniques and QuEChERS, for a greater method validation [58, 69, 71, 73].

Table 2. Chromatographic determination of FB1[1]

Support	Method	Eluent	Measurement	Assay Time (min)	Limit of Detection	Sample	Fumonisin Type	Ref
Wakosil 5C18 column	HPLC	Acidified methanol and disodium phosphate (80:20 pH 3.3)	Fluorescence	24	50 &100 µg/Kg	Corn	FB1, FB2, FB3	[38]
Synergi Max-RP (80 Å, 5 µm, 250 × 4.60 mm) HPLC column	HPLC	Methanol/0.1 M phosphate buffer (77:23, v/v) adjusted to pH 3.35 with concentrated orthophosphoric acid.	Fluorescence	-	25 µg/Kg	Corn kernels, tortillas and masa	FB1	[39]
Luna C18 column (50 × 4.6 mm ID, 5 µm Phenomenex)	LC-MS	Water/acetonitrile/formic acid at	MS detection	11	0.02 µg/L	Urine (Tortilla consumption)	FB1	[40]
Column C18 XTerra Waters narrow bore with a C18 precolumn cartridge;	LC	Acidified water & methanol	MS/MS analysis	50	5 µg/kg	Corn	FBs,HFBs	[41]
Column, C18 Hypersil	LC	Acidified water & acetonitrile	MS/MS analysis	13	16 µg/kg	Corn	HFBs	[41]
Gemini® C18 column	HPLC	Methanol/water/acetic acid with ammonium acetate	MS/MS analysis	21	8 µg/kg	Corn	HFBs	[41]
Column Brownlee C18	HPLC	Water–acetonitrile–acetic acid	Fluorescence	-	100 µg/kg	Corn	FBs	[41]
Symmetry Spherisorb ODS2 C18 Column	HPLC	Methanol& sodium dihydrogen phosphate	Fluorescence	11.20	50 µg/kg, 70 µg/kg	Tunisian foods and feed	FB1, FB2	[42]
XTerra MS C18 column	LC-MS-MS	Acidified water:acetonitrile & acetonitrile	MS-MS detection	<4 min (LC-ESI-MS/MS signal)	0.003 µg/kg	Bovine Milk	FB1	[43].
Luna C18 column	LC-MS-MS	Acidified water & methanol	MS-MS detection	25	5 µg/L	Urine	FB1,FB2	[44]
Agilent Zorbax Eclipse XDB C- 18 column	LC-MS/MS	Acidified water & methanol	MS	15	9, 6 µg/kg	Maize	FB1,FB2	[45]
Hypersil™ ODS C18 Columns	HPLC	Acetonitrile & sodium phosphate buffer	Fluorescence	~13.5 (retention time)	50 µg/kg	Rice	FB1	[46]
Shimadzu C18 column	HPLC	Water/acetonitrile/acetic acid	Fluorescence	-	30 µg /kg	Corn	FB1	[47]
Thermo Hypersil GOLD column	LC-MS	Acidified water & acetonitrile	MS detection	6	3.3 µg /kg	Human hair	FB1	[47]
SHISEIDO Capcell core C18 column	UFLC	Acetonitrile -water (0.1% formic acid)	MS/MS	12	0.15 µg/kg	*Areca catechu*	FB1, FB2	[48]
SHISEIO Capcell coreC18 column	UFLC	0.1% formic acid in acetonitrile and water	MS/MS	12	0.05 µg/L 0.15 µg/L	Yam	FB1, FB2	[49]
ACQUITY UPLC BEH C18 column	UHPLC	Water containing 0.1% formic acid (ESI+) or 0.1% ammonia (ESI-) and acetonitrile	MS	12	0.32 µg/kg, 0.08 µg/kg	Radix Paeoniae Alba	FB1, FB2	[50]
ZIC-pHILIC (SeQuant)	LC	Aqueous ammonium formate	MS	23	0.3, 1.3, 1.3, 0.8, 0.9, 2.6 µg/kg	Apples, apricots, lettuce, onion, wheat flour, chickpeas	FB1	[51]
Poroshell 120 PFP column	UHPLC	Ammonium formate and formic acid in Milli-Q water and methanol (ESI+), and Milli-Q water and acetonitrile (ESI−).	MS/MS	17	1, 1, 3 µg/kg	*Pheretima*	FB1, FB2, FB3	[52]
Kinetex C18 column	LC	Water-methanol with ammonium formate and formic acid	MS/MS	33	1.7, 3.9 µg/L	Maize	FB1, FB2	[53]
CORTECS C18 column	UPLC	Methanol-water with 0.5% (v/v) formic acid	MS/MS	30.3	15 µg/kg	Cereals (Wheat, corn, and rice)	FB1,FB2,FB3	[54]
Acclaim 120 C18 analytical column	HPLC	Acidified acetonitrile	Fluorescence	30	30 µg/kg 2.5 µg/L	Corn based feed	FB_1,FB_2	[55]
BEH C18 column	LC-MS-MS	Acidified water & acetonitrile	MS-MS detection	2, 4 (only hair)	0.014, 0.040, 0.012, ND µg/L	Pig plasma, urine, feces, hair	FB_1	[56]
Nucleodur C18 Gravity SB column	LC	Acetonitrile (2% acetic acid)- water (0.1% acetic acid)	MS	11.5	0.521 µg/L	Human blood	FB1	[57]
Ascentis Express C18	LC	Aqueous ammonium formate (0.1% formic acid)-aqueous methanol solution (ammonium formate, + formic acid, 0.1%)	MS/MS	30.1	10.14, 2.5, 0.625 µg/L	Milk	FB1, FB2, FB3	[58]
MNPs + Acquity UPLC®BEH C18 column	UPLC	MeOH/H_2O (60:40) with ammonium acetate and formic acid	MS/MS	10	0.210 µg/kg	Vegetable oil	FB1	[59]
Kinetex XB-C18 100 Å column	HPLC	Methanol- water (with ammonium formiate+ formic acid)	MS/MS	30	100 µg/kg	Cereal-derived products	FB1, FB2	[60]
Cortecs UHPLC C18 column	LC	Water-MeOH (with NH_4HCOO+ HCOOH)	MS/MS	14.5	0.04 µg/L	Soy, oat and rice beverages	FB1,FB2	[61]
Gemini® C18 column	LC	Methanol/water/acetic acid 10:89:1 (v/v/v) -97:2:1 (with ammonium acetate)	MS/MS	20.5	3.2 (FB1), 2.4 µg/kg	Maize-*fufu*	FB1,FB2, FB3, FB4, FA1	[62]
C18 column	UHPLC	Water- MeOH with formic acid and ammonium formate	MS/MS	11.25	17.3,12.4,10.7, 9 µg/L (FB1), 11.8,17.2, 9, 10 µg/L (FB2)	Oat, soy,rice and bird seed milk	FB1,FB2	[63]
Acquity BEH C18 column	UPLC	Water (ammonium acetate)- MeOH (formic acid)	MS/MS	15	0.20, 0.15 µg/kg	*Alpinia oxyphylla*	FB1,FB2	[64]

Eclipse Plus C8 RRHD column	MA-D- µ-SPE with UHPLC-Q-TOF/MS	Water containing 0.1% formic acid-acetonitrile	MS	9	0.0068, 0.013, 0.0074, 0.0030 µg//kg	Peach seed, milk powder, corn flour	FB1	[65]
C18 column Phenomenex Kinetex	UPLC-MS/MS	Water containing 0.5 mM NH_4Ac - MeOH with 0.1% formic acid	MS/MS	15	0.25 & 0.1 (FB2) µg//kg	Lotus seed	FB1, FB2	[66]
ZORBAX RRHD Eclipse Plus C18	UHPLC	0.1% formic acid solution - acetonitrile (formic acid)	MS	12	1 µg/L	Grape and wines	FB1	[67]
Gemini® C18-column	LC	Methanol/water (with acetic acid and ammonium acetate	MS/MS	-	1 µg/kg	Dried date palm fruits	FB2	[68]
Acquity UPLC HSS T3 column	UPLC	(Formic acid & ammonium formate) water-acetonitrile	MS/MS	10	0.15, 0.09, 0.04, 0.03, 0.17 µg/L	Broiler chicken plasma	FB1, FB2, pHFB1a, pHFB1b, HFB1	[69]
Silica based particles bonded with C18-penta fluorophenyl functions	LC-HRMS	Water- acetonitrile (both with formic acid) - MeOH	MS	26	0.5 µg/L	Tea	FB1, FB2	[70]
Gemini-NX LC-column	LC	Water - methanol acidified (both with ammonium formate +formic acid)	MS/MS	39	1.5, 0.3 (vegetables) µg/kg	Ready-to-eat food (cereals, fish, legumes, vegetables, meat)	FB1, FB2	[71]
Scherzo Sm-C18 column	HPLC	Acetonitrile (ammonium acetate) - acetonitrile (formic acid)	MS/MS	26	2.4, 2.3 µg/kg	Corn derived products	FB1, FB2	[72]
Acquity HSS T3 column	LC	Water-ACN (both acidified with HAc)	MS/MS	25	0.001 µg/L	Human urine	FB1	[73]
Waters ACQUITY HSS T3 column	UPLC	0.1% formic acid and 5 mM ammonium formate (phase A) -methanol (phase B).	MS/MS	13	0.22 µg/L	Beer	FB1, FB1	[74]
Zorbax CX	UHPLC	Methanol/water (1:1 v/v) with 0.1% acetic acid	MS/MS	3.6 (chromatogram time)	51.5, 45.3 µg/kg	Rice	FB1, FB2	[75]
Kinetex Core-shell C18	LC	Water- methanol (both with ammonium formate and formic acid)	MS/MS	25.5	8.3 µg/kg	Green coffee	FB1, FB2	[76]
Kinetex Biphenyl column	LC	0.01 M ammonium acetate + 0.1% of acetic acid in water/ MeOH - 0.01 M ammonium acetate+ 0.1% of acetic acid in water/MeOH	MS/MS	16	0.50, 1.56 µg/kg	Animal feed	FB1, FB2	[77]
UPLC HSS T3	LC	Aqueous ammonium formate 1mM and formic acid 1% (phase A)-Ammonium formate 1mM and formic acid 1% in methanol:water(95:3.9)	MS/MS	11	20 µg/kg	Nixtamalized Maize	FB1, FB2	[185]
Kinetex 2.6 µm C18 100A	UHPLC	Aqueous acetic acid 0.5% (phase A)-Acetic acid 0.5% and isopropanol 99.5% (phase B)	MS/MS	11	0.03, 0.01 µg/L	Kankankan	FB1, FB2	[186]
Gemini C18-column	LC-ESI	Ammonium acetate 5 mM with methanol/water/acetic acid 10:89:1 (phase A) and 97:2:1 (phase B)	MS/MS	18.5	2.39, 1.68, 8.55 µg/kg	Dried Turkish figs	FB1, FB2, FB3	[187]

[1] Abbreviations: **HRMS:** High-resolution mass spectrometry; **SPE:** Solid-phase extraction; **UFLC:** Ultra-fast liquid chromatography; **UHPLC:** Ultra-high-performance liquid chromatography

3.2 Immunosensors for detection of fumonisin

The enzyme-linked immunosorbent assay (ELISA) for the determination of FB1 represents the foundation of different approaches. Competitive assays have been commonly employed for biosensing techniques, mostly because of the restriction produced by single epitopes on other types such as sandwich ELISA [85]. Some general procedures for a competitive immunoassay include a coating stage of antibody on the selected support, followed by the incubation with a mixture of free FB1 (sample) and functionalized toxin (horseradish peroxide (HRP)-FB1). After washing the unbound FB1 or HRP-FB1, different substrates can be added for the development of either a chemiluminescence or a colorimetric signal [86]. Some commercial kits are also based on a competitive scheme, in which capture antibodies, specific to a FB1 antibody, are coated on a well, where free FB1, enzyme-fumonisin and antibody are incubated. The bound HRP-fumonisin is then measured by incubating with a chromogen [42]. In some bulk experiments, magnetic nanobeads have been used as a support with a competitive binding role under the presence of FB1 and its biotinylated antibody [137].

Other modifications suggested the substitution of HRP with compounds such as glucose oxidase to produce hydrogen peroxide, an inducer of AuNP aggregation [133], and the application of genetically engineered antibodies [138]. A novel technique used a monoclonal antibody-rhodamine isothiocyanate (RBITC)-AuNPs probe for the competitive binding between OVA-FB1 and FB1, where cysteamine worked as a turn-on compound for revealing the degrees of fluorescence from the quenched probe [188].

This antigen-antibody interaction has been used, optimized and improved over the years; and commercially available ELISA kits and standardized ELISA protocols are still applied for method validation and comparison with novel biosensing developments [128, 130, 143, 166, 170]. As presented in Fig 4, electrochemical immunosensors have portrayed some of the lowest LODs [101,109]. For instance, the signal of an impedance sensor was modified by depositing quantum dots-carbon nanotubes on a glassy carbon electrode (GCE) for the immobilization of the corresponding antibody. In this case, the electron transfer resistance was enhanced after target binding, allowing LODs as low as 0.46 pg/L [101]. An electrochemical indirect competitive method was also refined by modifying a GCE with nanotubes-chitosan (undefined characteristics) and FB1-Bovine serum albumin (BSA). The remaining antibody after the incubation with free FB1 (sample) was able to bind FB1-BSA, as well as an alkaline phosphate-labelled anti-antibody, whose substrate triggered the electrochemical signal with lower, yet good sensitivity of 2 ng/L [103]. The reduction of conductivity promoted by the antibody-antigen reaction was again explored for the immobilization of antibodies on nanotube-modified GCE, attaining a LOD of 3.8 pg/L [109]. In addition to electrochemical methods, surface-enhanced Raman scattering (SERS) competitive immunoassays were applied by combining FB1-BSA functionalized Au nanopillars with nanotags, consisting in AuNP simultaneously functionalized with anti-antibody and malachite green isothiocyanate (MGITC). The interaction between the primary antibody and high antigen concentrations resulted in a weak SERS signal, due to the absence of complex formation within free primary antibodies, nanopillars and nanotags, with a LOD of 0.00511 pg/L [126].

As noted in Table 3, immunosensors can be supported on different matrices, including optical fiber, well plates, glass slides, magnetic beads, magnetic nanoparticles, electrodes and chips. Yet another of the main advantages of using antibodies is the feasibility to be incorporated in paper-based biosensors. Paper matrices are presently relevant for the creation of portable, point-of-care, applicable and cheap devices [36]. The conjugation of antibodies with colloidal gold (gold nanoparticles) has been widely applied for the colorimetric detection of FB1 on nitrocellulose membranes [88, 91, 94, 95, 98, 99, 102, 107, 113, 116, 120, 136]. Some modifications included the application of urchin-like and flower-like gold nanoparticles (AuNP), which slightly increased the sensitivity when compared to a spherical particle [107, 135].

Table 3. Immuno-based assays for the determination of FB1[1]

Support	Method	Labelling/Substrate	Measurement	Assay Time (min)	LOD	Sample	Fumonisin	Ref
96-well immunoplates	ELISA	HRP	Optical density	150	0.2 µg/L	Corn	FB1	[38]
ELISA kit	AgraQuant Total Fumonisin Assay Protocol	Methanol-water	Intensity of colour	20	200 µg/kg	Corn	FBs	[41]
96-well plate	ELISA (RIDASCREEN ®)	HRP	Optical density	55	25 µg/kg,	Tunisian foods and feed	FB1+FB2	[42]
Test kit	ELISA	Antigen	OD	20	200 µg/kg	Maize	FB1+FB2	[45]
Optical fibre	DC assay	FITC	Fluorescence	24	10 µg/L	Corn	FB1	[81]
Sample cell	SPR	Gold film	Reflected light intensity	10	50 µg/L	PBS	FB1	[82]
Protein-A coated capillary column	Liposome-amplified competitive assay	Liposome	Fluorescence	<11	1 µg/L	TBS	FB1	[83]
Glass culture tube	Competition of unlabelled fumonisin	Fluorescein	Fluorescence Polarization	2	500 µg /kg	Maize	FB1	[84]
Borosilicate glass slides	Competitive assay	Biotin	Fluorescence	~8	250 µg/L	PBSTB	FB1	[85]
96-well microplate	ECL-ELISA	HRP	Fluorescence	60	0.09 µg/L	Cereals	FB1	[86]
DMA-NAS-MAPS treated glass	Competitive immunoassay	Streptavidin-AP/ NBT/BCIP	Colorimetric	65	43 µg/L	Binding buffer	FB1	[87]
NC membrane	LFIA	Colloidal Gold	Line intensity	4	199 µg/kg	Maize	FB1	[88]
Luminex 100 microspheres	Indirect competitive fluid array	Biotin	Fluorescence cytometry	60	0.3 µg/L	Grain Products	FB1	[89]
SPGE	DC assay	HRP-TMB	Chronoamperometry	45	5 µg/L	Corn	FB1,FB2	[90]
NC membrane	LFIA	Colloidal Gold	Line intensity	10	120 µg/L	Maize	FB1	[91]
Aldehydelized glass slides	Specific competitive reactions	Ag conjugates	Fluorescence	90	109.06 µg/L	Wheat	FB1	[92]
NC strip	Competitive lateral flow immunoassay	HRP	CL	15	2.5 µg/L	Maize	FB1,FB2	[93]
NC membrane strip	One-step competitive immunochromatographic	AuNP	Colour density	10	2.5 µg/L	Maize	FB1+FB2+FB3	[94]
NC membrane	LFIA	Protein A-gold	Line intensity	30	3200 µg/kg	Maize	FB1	[95]
96-well microplate	IC ELISA	HRP	Absorbance	70	8.32 µg/kg	Corn	FB1	[96]
Paramagnetic beads	Inhibition immunoassay	Mycotoxin-R-Phycoerythrin	Dose–response cytometry (Fluorescence)	50	170, 1270 µg/kg	Maize, wheat	FB1+FB2	[97]
NC membrane	LFDIA	Colloidal Gold	Line intensity	30	5.23 µg/L	Corn	FB1	[98]
NC membrane	Immunochromatographic strip	Colloidal gold	Visual detection	3	5 µg/L	Cereal	FB1	[99]
PrG functionalized magnetic beads	DC multi-channel electrochemical immunoassay	HRP	Current	40	0.58 µg/L	Cereals	FB1	[100]
SPCEs GCE/PT	Impedimetric immunosensor	PDMA-MWCNT	EIS	-	0.00000046 µg/L	Methanol	FB1	[101]
					14 µg/kg	Corn	FB1	
					11 µg/kg	Corn	FB2+FB3	
NC strip	LFIA	HRP	CL	30	6 µg/kg	Maize	FB1	[102]
SWNTs/CS electrode	Indirect competitive binding	Alkaline phosphatase	Electrochemical	180.11	0.002 µg/L	Corn	FB1	[103]
SPCEs-Magnetic beads	Competitive multi- immunoassay	HRP	Amperometric	60	0.33 µg/L	CRM, beer	FB1,FB2,FB3	[104}
96-well microplate	Biopanning	Ab2β Nb /HRP	OD	~60	0.15 µg/L	PBS	FB1,FB2	[105]
Microplate reader	FPIA	FITC	Fluorescence Polarization	<30	157.4, 290.6 µg/kg	Maize	FB1, $FB2_2$	[106]
NC membrane	Competitive small molecule detection	UGNs	Colour intensity	<5	5 µg/L	Grains	FB1	[107]
NC membrane	Competitive small molecule detection	AuNP	Colour intensity	<5	20 µg/L	Grains	FB1	[107]
PPy/ErGO SPE	Label-free electrochemical immunosensing	AuNP	Current	40	4.2 µg/kg	Corn	FB1	[108]
GCE	Electrochemical impedance spectroscopy	PDMA-MWCNT	Electron transfer resistance	-	0.0000038 µg/L	Corn	FB1	[109]
NC membrane	Immunochromatographic strip test	DR-AuNP	Visual detection	10	1000 µg/kg	Maize flour	FB1	[110]
Hi-Flow Plus membranes	Competitive reaction	AuNP	Coloration	15	0.6 µg/L	Maize	FB1	[111]
Microbead	Flow immunocytometry	Phycoerythrin	Fluorescence	45	116 µg /kg	Maize	FB1	[112]
NC strips	Competitive assay	Colloidal gold	Colour intensity	10	0.24 µg/L	Agricultural products	FB1	[113]
Plates	IC ELISA	IgG-HRP	Absorbance	68	0.08 µg/L	Agricultural products	FB1	[113]
Mimotope on ARChip Epoxy slides	Competitive binding inhibition	Alexa Fluor 647- IgG	Fluorescence	210	11.1 µg/L	Maize, wheat	FB1	[114]
NC high-flow plus membranes	Competitive binding inhibition	AuNP/ HRP-labelled IgG	Colour	10	25 µg/L	Corn	FB1	[115]
Nitrocellulose membrane	LFIA	AuNP/ CdSe/ZnS QD	Fluorescence	15	62.5 µg//kg	Maize flour	FB1, FB2	[116]
96-well microplates	Competitive assay	AuNF@FeTPPCl + TMB	Colour	40	0.05 µg/L	Buffer	FB1	[117]
Mycotoxin-protein conjugates on chip (MZI)	Primary (mycotoxin/protein conjugates - anti-mycotoxin specific mAbs) and secondary immunoreaction (immune adsorbed mAbs- IgG antibody)	Label-free	Phase shift	12	5.6 µg/L	Beer	FB1	[118]

96-well plates with protein G-coated AuNPs (bulk)	Competitive immunoassay	YFP-tagged FB1-mimotope	Fluorescence	45	1.1 µg/L	Wheat	FB1, FB2	[119]
NC membrane	Competitive inhibition reaction	Antibody- AuNP conjugates, FB1-BSA, IgG	Visual detection	10	30 µg/L	Corn	FB1	[120]
Anti-FB1 mAbs on plate well	Competitive fluorescence ELISA	CAT-regulated-fluorescence quenching of MPA-QD	Fluorescence	75n	0.33 µg/L	Corn	FB1	[121]
Gold coated magnetic NP	Competitive CLIA	HRP-LUMINOL	Fluorescence	150	0.027 µg/L	Cereals	FB1	[122]
Microplate	IC-ELISA	IgG-HRP	Absorbance	120	0.078 µg/L	Corn	FB1,FB2,FB3	[123]
Microplate	DC-pELISA	AuNP	Absorbance	120	12.5 µg/L	Corn	FB1	[124]
Test column	IATC	HRP	Color intensity	5.5	20 µg/kg	Maize	FB1,FB2,FB3	[125]
Au nanopillars	Surface-enhanced Raman scattering	Malachite green isothiocyanate-AuNP	Raman intensity	120	0.00511 pg/mL	Standard curve	FB	[126]
NC membrane	Direct competition	Streptavidin-horseradish peroxidase	Enhanced chemiluminescence	45	0.24 µg/L	Corn samples	FB1	[127]
Anti- FB1 mAb in microtiter wells	Non-competitive idiometric nanobodies phage ELISA	HRP conjugated anti-M13 antibody-TMB	Absorbance	130	0.19 µg/L	Corn	FB1	[128]
ITO coated glass integrated with PDMS microfluidic channel.	Three-electrode electrochemical sensor	AuNP-Ab	Current	50	0.097 µg/L	Corn	FB1	[129]
Superparamagnetic carboxylated xMAP® microspheres	Quadplex FCIA	R-PE conjugated goat anti-mouse antibody	Fluorescence	60	2.45 µg/L	Milk	FB1	[130]
NC membranes	Multiplex ICr assay	QD nanobeads	Fluorescence	10	20 µg/L	Maize	FB1	[131]
GONC on DEP electrodes	Electroactivity reduction with biorecognition.	Label-free	CV/DPV	65	294 µg/L	PBS-T	FB1	[132]
96 well plates with protein-G and BSA	Competitive Plasmonic ELISA	Glucose oxidase-FB1	Absorbance	180	0.31 µg/L	Maize	FB1	[133]
NC membrane	Competitive multiplex ICr Assay	Quantum dot nanobeads-MAb	Fluorescence (test line/ control line)	18	1.58 µg/L	Cereals	FB1	[134]
NC membrane	ICr strip	Flower-like AuNP	Color intensity	5	5 µg/L	Chinese traditional medicine	FB1	[135]
NC membrane	Multiplex ICr test	AuNP	Colour intensity	-	60 µg/L	Wheat and corn	FB1	[136]
Nanomagnetic beads	Competitive solid-phase assay	Biotin NHS-Streptavidin-HRP	OD	22	0.21 µg/L	Maize	FB1	[137]
NC membrane	Competitive ICr strip	Colloidal gold-scFv	Color Intensity	10	2.5 µg/L	Maize	FB1	[138]
NC membrane	Smartphone-based multiplex LFIA	AuNP and TRFMs	Ratio T/C line color & fluorescence	8	0.59 µg/kg (C) 0.42 µg/kg (F)	Maize, wheat, bran	FB1	[139]
Microplate-OVA-FB1	Competitive immunoreaction	Cysteamine on mAb-RBITC-AuNPs	Fluorescence	46	0.023 µg/L	Maize	FB1, FB2, FB3	[188]
NC membrane	Competitive ICr strip	QDNBs-mAb	Fluorescence	25	60 µg/L	Wheat. corn	FB1	[189]
NC-membrane	Immunochromatographic assay	Eu-FM-mAB	Time-resolved fluorescence	7	8.26 µg/kg	Corn, corn flour, wheat, rice, brown rice	FB1	[190]

[1] Abbreviations: **Ab2β Nb:** Anti-idiotypic nanobody; **AP/NBT/BCIP:** Alkaline phosphatase/ nitro blue tetrazolium chloride/5-Bromo-4-chloro-3-indolyl phosphate toluidine salt; **AuNP**: Gold nanoparticles(spherical)**; BSA:** Bovine serum albumin; **CAT:** Catalase; **CL:** Chemiluminescence; **CLIA:** Chemiluminescence immunoassay; **CV:** Cyclic voltammetry; **DC:** direct competitive; **DEP:** Disposable electrical printed; **DMA-NAS-MAPS**: Copoplymer (N,Ndimethylacrylamide)- N,N-acryloyloxysuccinimide-[3-(methacryloyl-oxy)propyl] trimethoxysilyl; **DPV:** Differential pulse voltammetry; **DR:** Desert rose-like; **ECL:** Enhanced chemiluminescent; **EIS:** Electrochemical impedane spectroscopy; **ErGO:** Electrochemically reduced graphene oxide; **Eu-FM:** Europium Fluorescent Nanosphere; **FCIA**: Flow cytometric immunoassay; **FeTPPC:** Iron porphyrins; **FITC:** Fluorescein isothiocyanate; **FPIA:** Fluorescence polarization immunoassay; **GCE:** Glassy carbon electrode; **GONC:** Graphene oxide nanocolloids; **HRP:** Horseradish peroxidase; **IATC**: Immunoaffinity test column; **IC:** Indirect competitive; **ICr:** immunochromatographic; **IgG:** Goat anti-mouse immunoglobullin; **ITO:** Indium tin oxide; **LFIA:** Lateral flow immunoassay; **mAb:** Monoclonal antibody; **MPA-QD:** mercaptopropionic acid-modified CdTe quantum dots; **MZI:** Mach-Zehnder interferometers; **NC:** Nitrocellulose; **NHS:** *N*-Hydroxysuccinimide; **NP:** Nanoparticles; **OD:** Optical density; **p:**plasmonic; **PDMA-MWCNT:** Poly(2,5-dimethoxyaniline) multi-walled carbon nanotube composite; **PDMS:** Polydimethylsiloxane**; PPy:** Polypyrrole; **PrG:** Recombinant Protein G; **QD:** Quantum dot; **QDNBs:** Quantum dots nanobeads; **RBITC:** Rhodamine B isothiocyanate; **R-PE:** R-phycoerythrin; **scFv:** single-chain variable fragment; **SPCEs:** Screen -printed carbon electrode; **SPE:** Screen-printed carbon electrode; **SPGE:** Bare gold screen-printed electrode; **SPR:** Surface plasmon resonance; **SWNTs/CS:** Single-walled carbon nanostructure/ Chitosan; **TMB:** 3,3',5,5'-tetramethylbenzidine dihydrochloride; **TRFMs:** Time resolved fluorescence microspheres; **UGNs:** Urchin-like gold nanoparticles; **YFP:** Yellow fluorescent protein

As an alternative to color intensity measurements, a chemiluminescent substrate could be incubated with HRP for a slight improvement of the LOD [93, 127], or the application of quantum dot (QD) in which a radiometric analysis revealed a constant signal from the test line with biotin-BSA, compared to the calibration with anti-mouse IgG [134]. Nevertheless, the application of fluorescent QDs not always result in an improved sensitivity, as reported for a nitrocellulose strip for the detection of FB1 (LOD: 60 µg/L) , ZEN and OTA with a monoclonal antibody-QD probe placed on the conjugate pad, through the competitive interaction with mycotoxin-BSA at the test line [189], and a mAB-Europium fluorescent nanoparticle with FB1 (LOD: 8.26 µg/L) and FB1-BSA (Test line) [190]. An advantage of paper-based biosensors is the possibility of performing smartphone-based analysis, as already achieved on colorimetric and fluorescent signals [139]. Notwithstanding the multiple modifications, most of the differences among paper-based and other types of immunosensors can be explained in terms of the different antibodies selected and employed in each method.

3.2 Other methods

Alternatives to the extensively known immunologic and chromatographic techniques include chemometric, electrochemical and colorimetric analysis, as shown in Table 4. In SERS, the spectral variations of extracted samples mixed with Ag dendrites were measured on a quartz plate [140], while innovative, promising and more robust techniques incorporated the use of molecularly imprinted polymer nanoparticles (MIPs). Commonly polymerized with monomers such as methacrylic acid (MAA), ethylene glycol methacrylate (EGMP), N-isopropylacrylamide (NIPAM), N,N'-methylene-bis-acrylamide (BIS), N-tert-butylacrylamide (TBAm), and N-(3-Aminopropyl) methacrylamide hydrochloride (NAPMA); MIPs have functioned as a replacement of primary antibodies; in which the utilization of FB1 as template molecule enhanced the performance, selectivity, thermal stability, and easy manufacturing of this technique. Once the MIPs are synthesized, the general procedure is similar to ELISA, where free FB1 competes with a FB1-HRP conjugate, where the latter reacts with a substrate (TMB: 3,3′,5,5′-tetramethylbenzidine), bearing a colorimetric response. Such mechanism reduces the limit of the detection to 4.4 ng/L [141] and 1.37 ng/L [143], while an improvement on the silanisation step yielded more MIPSs and allowed the quantification of FB in maize, with a lower LOD equivalent to 1 ng/L [145]. Recent alternative methods suggested the chemical modification of FB1 prior to its quantification assay, where alkaline hydrolysis with KOH was proposed to reduce steric hindrance, allowing the formation of hydrogen bonds between hydrolysed fumonisin (HFB1) and the NH_2 groups in cysteamine functionalized AuNP [146]. Likewise, a derivatization step between FB1 and a fluorescent derivative was necessary for spectra acquisition on a nylon membrane [146]. Besides, as already observed for some immunoassays, electrochemical methods were combined with MIPs, for a reduction on the limit of detection. A GCE modified with AuNPs and $Ru@SiO_2$ in chitosan (undefined characteristics), was proved as favorable support to produce MIPs generating electrochemiluminescent estimations with a LOD of 0.35 ng/L [142]. In a similar approach, an iridium tin oxide (ITO) electrode modified with CdS quantum dots, chitosan (undefined characteristics) and graphene oxide worked as the UV polymerization area, in which the resulting MIPs were used for photoelectrochemical evaluation of FB1 levels as low as 4.7 ng/L [144]. The application of nanoMIPs in electrochemical measurements (EIS, DPV) allowed the achievement of LODs as low as 21.6 fg/L, which so far is the lowest value reported for FB1 [191].

On the other hand, capillary electrophoresis (CE) was initially reported in 1995 as a different technique with greater capability for the separation of FB1 to that from LC, where either its integration with MS detection or the quantification of fluorescent derivatives were utilized in the analysis of corn [192, 193]. Subsequent CE approaches explored the performance of fluorescein isothiocyanate for the derivatization of FB1 [194], and its application in the competitive binding of mAb by labeled (derivatized) and unlabeled FB1, for the CE of the remaining fluorescein-FB1 [195]. Despite the advantages of CE in terms of the column efficiency, speed, reduction of organic solvents [193], the high limit of detections restricted any further applications. After two decades only one recent work on the application of coated (C_1) and uncoated capillaries resulted in a relatively high LOD of 156 µg/L for the analysis of rice and fusarium microconidia by CE-MS [196], which denotes an opportunity for exploring, refining and optimizing more CE options for the determination of FB1 and other analogues.

Table 4. Other methods for FB1 determination [1]

Support	Method	Labelling/ Substrate	Bioreceptor	Measurement	Assay Time (min)	LOD	Sample	Fumonisin Type	Ref
Quartz plate	Surface-enhanced Raman spectroscopy	Ag Dendrites	SPR	Raman signal	<1	>5000 µg /kg (not reported as LOD)	Maize	FB1,FB2, FB3	[140]
Polymer-coated microplates	MIP	HRP-conjugate	nanoMIPs	Absorbance	70	0.0044 µg/L	PBS	FB2	[141]
GCE-AuNPs-Ru@SiO_2-Chitosan	SEECL	MIP containing FB1 + MAA+ EDMA+AIBN	MIP-Amino group	ECL	5	0.00035 µg/L	Milk, maize	FB1	[142]
96-well microplates+EGMP, NIPAm, NAPMA, TBAm	Direct competitive assay based on	HRP–FB1 conjugate + TMB	MINA	Color	5.16	0.00137 µg/L	PBS buffer	FB1	[143]
ITO electrode surface coated with GO/CdS/CS	MIP-Photoelectrochemical sensor	MIP including FB1, MAA, EDMA and AIBN	MIP	Photocurrent	15	0.0047 µg/L	Maize meal and milk	FB1	[144]
Polymer-coated microplates (EGMP,NIPAm,BIS, NAPMA)	MINA	HRP-conjugate + TMB	nanoMIPs	Absorbance	70	0.001 µg/L	Maize	FB1	[145]
Cys-AuNPs	Aggregation based colorimetric detection	AuNPs	HFB1	Absorbance	65	0.90 µg/kg	Corn	FB1	[146]
Syringe SPE (Nylon membrane)	Solid-phase fluorescence spectrometry	RhB-Cl	Derivatization	Relative Intensity (Fluorescence)	4	0.119 µg/L	Maize	FB1	[147]
nanoMIPSs-PPy/ZnP-Pt Electrode	Electrochemical sensor	MIP+FB1+NIPAM+BIS+TBAm+EGMP+NAPMA	MIP	EIS, DPV	5	0.0000000216, 0.0000005 µg/L	Maize	FB1	[191]
Fused silica capillary	CE	Ammonium formate/ammonia+ ACN 10% (Background electrolyte)	-	MS	40	156 µg/L	Rice, *Fusarium* microconidia	FB1, FB2	[196]

[1]Abbreviations: **ACN:** Acetonitrile; **AIBN:** Azodiisobutyronitrile; **AuNP:** Gold nanoparticles; **BIS:** N,N'- methylene-bis-acrylamide; **CE:** Capillary electrophoresis; **Cys-AuNPs:** Cysteamine-capped gold nanoparticles; **DPV:** Differential pulse voltammetry; **ECL:** Electrochemiluminescence; **EDMA:** Ethylene glycol dimethacrylate; **EIS:** Electrochemical impedance spectroscopy; **EGMP**: Ethylene glycol methacrylate; **GCE:** Glassy carbon electrode; **GO:** graphene oxide; **HFB1**: Alkaline hydrolysis of FB1; **HRP:** Horseradish peroxidase; **ITO:** Indium tin oxide; **MAA:** Methacrylic acid; **MINA:** Molecularly imprinted polymer nanoparticles; **MIP:** Molecularly imprinted polymer; **NAPMA:** N-(3-Aminopropyl) methacrylamide hydrochloride; **NIPAm:** N-isopropylacrylamide; **PPy/ZnP:** Polypyrrole-zinc porphyrin; **RhB-Cl:** 9-[2-(Chlorocarbonyl)phenyl]-3,6-bis(diethylamino) xanthylium; **SEECL:** Surface-enhanced electrochemiluminescence; **SPE:** Solid Phase Extraction; **SPR:** Surface plasmon resonance; **TBAm:** N-tert-butylacrylamide; **TMB:** 3,3′,5,5′-tetramethylbenzidine

4 Aptamer-based determination of FB1

Aptamers are single-stranded DNA or RNA with high molecular recognition towards different types of molecules. Such probes exhibit diverse binding affinities and target selectivity and can discriminate even slight chiral differences. Aptamers are selected by a technique called Systematic Evolution of Ligands by Exponential enrichment (SELEX) in which a DNA library is incubated with the target or other relevant molecules, followed by the amplification of potential binders after several selection and discrimination rounds [148]. So far, two aptamers composed by 96 and 80 nucleotides, have been reported through SELEX and utilized in different biosensing approaches [148, 149], all the aptamer-based sensors are chronologically described in Table 5, while the binding and functionalization conditions are illustrated in Table 6. From the 31 aptasensors found in the literature, 24 utilized the 96 nt aptamer [148], one method applied a shortened version (60 nt) from this first sequence [159], one platform included the second 80 nt aptamer[156], two biosensors manipulated a condensed version (40 nt) of the second main aptamer [164, 167], and three references did not specify their single-stranded (ss) DNA sequence [175,177,198]. The schematic representation of each type of aptasensor assay is illustrated in Fig 6a a for the biosensors involving the initial 96 nt aptamer, and in Fig 6b for the application of the subsequent and not specified aptamers. It should be noted that the most recent sequences have not replaced the first reported aptamer, and current biosensing designs still apply the 96 nt ssDNA molecule with high sensitivity and specificity.

Table 5. Aptasensors for the determination of FB1[1]

Support	Labelling	Measurement	Detection Time (min)	Extraction Time (min)	Sample Preparation Steps	LOD µg/L	Sample	Specificity Test[2]	Ref
GO	UCNPs with Er and Tm	Fluorescence spectra	200	-	-	0.1	PBS	**OTA**, AFB1, AFB2, AFG1, AFG2, FB2, ZEN	[151]
Carboxilated MNPs/MB	UCNPs	Fluorescence	100	>2	7	0.01	Maize	-	[152]
Centrifuge tubes	AuNP-cDNA	Absorbance	35	30	3	0.125	Beer	-	[153]
SPCMs	FITC-Complementary DNA	Fluorescence	60	135	3	0.00016	Cereal	AFB1, **OTA**, FB2	[154]
cDNA modified Au electrode	Au NPs–Ir	ECL	120.41	-	5	0.27	Wheat flour	OTA, AFT, L-cystein, BSA	[155]
GCE-AuNPs	Label free	EIS	30	745	8	0.0014	Maize	AFB1, ZEN, T-2 toxin	[156]
Au coated silicon cantilever beams	Label Free	Deflection	30	-	-	33	Buffer	OTA, DON	[157]
GCE-AuNPs-capture DNA	GS-TH	CV	25.11	-	-	0.001	Ultra-pure water	AFB1, OTA, ZEN, DON	[158]
cDNA (Corning® Costar® 96-Well Cell Culture Plates)	PicoGreen	Fluorescence intensity	25	-	2	0.1	Milk	CTN,OTA, AFB1, ZEN	[159]
SPCE- PDMS microcell	AuNPs	Impedance signal	30	735	7	0.0034	Corn	FB2, OTA, AFB1	[160]
SPCM	cy3 modified aptamer	Fluorescence	90	751	7	0.01104	Cereals	AFB1, **OTA**	[161]
SiO_2 spheres/ Fe_3O_4@Au Magnetic Beads-cDNA	PbS QD	SWV (current)	65	15	4	0.02	Maize	**OTA**, OTB, AFB1	[162]
Reduce graphene/Ni/ Pt NPs micromotors	Fluorescein amidine (FAM) labelled aptamer	Fluorescence intensity	15	Maize: 30 Beer: 20 Whine: -	4,1,1	0.4	Maize, Beer	**OTA**	[163]
Graphene modified GCE	Label free	Impedimetric signal	30	-	-	0.0123	Tris buffer	-	[164]
Centrifuge tube	FITC-Complementary DNA	Fluorescence	21	-	-	7.21	Buffer	AFB1, AFB2, OTA, FB2 (response)	[165]
TiO_2 modified porous silicon	Cy3 labelled aptamer-BHQ2 labelled anti aptamer	Fluorescence Intensity	720	751	7	0.00021	Cereal (Rice, Wheat, Corn)	**OTA, AFB1**	[166]
GONC on DEP carbon electrodes	GONC	Peak current intensity	65	-	-	10.82	Tris buffer	OTA, Thrombin	[167]
Reduced graphene/ Pt NPs micromotors	FAM labelled aptamer	Fluoresecence	17	30, 20	3,2	0.70	Maize. Beer	**OTA**	[168]
GO-cDNA (probe1)& Fe_3O_4/GO-cDNA (probe 2)	Allochroic dyes (thymolphthalein)-alkaline conditions	Absorbance	90	40	7	100 (lowest value explored)	Peanut	**OTA, AFB1, microcystin-LR**	[169]
Amine funtionalized Fe_3O_4 magnetic particles	$NaYF_4$: Ce/Tb nanoparticles-cDNA	Fluorescence decrease	60	>2	7	0.000019	Maize	**OTA** T-2, AFB1, OTB, ZEN	[170]
GO/Fe_3O_4 nanocomposites	Aptamer-Red QDs	Fluorescence inensity	60	-	3	0.0162	Peanut	OTA, **AFB1**, OTB. AFM1, AFB2	[171]
cDNA on AuE	Methylene blue	Peak current	40	45 (Corn)	3 (Corn) 1	0.00015	Corn Beer	OTA, ZEN, AFB1	[172]
MoS2-Au modified GCE	FC6S -Au-cDNA	Current difference	15	-	-	0.0005	PBS	**ZEN** α-ZOL, AFB1, DON, T-2, OTA	[173]
cDNA on AuE	AuNRs-Fc	DPV	10	-	4	0.00026	Beer	**OTA**, ZEN, AFB1	[174]
cDNA on AuNR	Cy5.5-aptamer	SERS/ Fluorescence	45	735	8	0.0003/ 0.0005	Corn	AFB1, ZEN, PAT, OTA, FB2, FB3	[175]
Streptavidin coated microplate	TMB	Absorbance	73	30	11	0.3	Beer Corn	AFB, DON, OTA, ZEN	[176]
cDNA2 on AuNR	UCNPs-Hibridized TAMRA-cDNA1& Aptamer	Fluorescence	50	735	7	0.000003	Corn	**ZEN**, AFB1, OTA, PAT, OTB	[177]
Aptamer-Magnetic Beads	cDNA-AgNP	Ag intensity (ICP-MS)	121	42	8	0.3	Wheat Flour	**OTA**, AFB1, DON, ZEN, FB2	[197]
Aptamer-AuNP-UCNP-AuNP-cDNA	4-MBA	SERS	121	735	9	0.00002	Corn	**ZEN, OTA**, AFB1, PAT, T-2	[198]
ITO electrodes	Silver-Au-Aptamer-cDNA-Fe_3O_4 & Prussian Blue	Color change of ITO (Mobile phone)	62	-	-	0.01	Corn	DON, OTA	[199]
AuNP	AuNP	UV-Vis	192.2	-	-	0.000056	$MgCl_2$ 1mM Buffer	OTA, AFB1	[200]

[1] Abbreviations: **AFB1:** Aflatoxin B1; **AFB2:** Aflatoxin B2; **AFG1:** Aflatoxin G1; **AFG2:** Aflatoxin G2; **AgNP:** Silver nanoparticles; **AuE:** Gold electrode; **AuNP:** Gold nanoparticles; **AuNRs:** Gold nanorods; **BHQ2:** Black hole quencher; **cDNA:** complementary DNA; **CTN:** Citrinin; **Cy:** Cyanine; **DEP:** Disposable electrical printed; **DON:** Deoxynivalenol; **DPV:** Differential pulse voltammetry; **FAM:** Fluorescein amidine; **FB2:** Fumonisin B2; **Fc:** Thiol modified ferrocene; **FC6S:** 6-(Ferrocenyl)hexanethiol; **FITC:** Fluorescein isothiocyanate; **GCE:** Glassy carbon electrode; **GO:** Graphene oxide; **GONC:** Graphene oxide nanocolloids; **GS:** Graphenes; **ICP-MS:** Inductively coupled plasma mass spectrometry; **ITO:** Indium Tin Oxide; **MB:** Molecular beacon; **MBA:** Mercaptobenzoic acid ; **MNP:** Magnetic nanoparticles; **MoS_2:** Molybdenum disulfide; **NP:** Nanoparticles; **PDMS:** Polydimethylsiloxane; **OTA:** Ochratoxin A; **OTB:** Ochratoxin B; **QD:** Quantum dots; **SERS:** Surface-enhanced Raman spectroscopy; **SPCE:** Screen-printed carbon electrode; **SPCM:** Silica photonic crystal microsphere; **TAMRA:** Carboxytetramethylrhodamine; **TH:** Thionine; **TMB:** 3,3′,5,5′-tetramethylbenzidine; **UCNPs:** Upconversion fluorescent nanoparticles; **ZEN:** Zearalenone; **ZOL:** Zearalenol; **PAT:** Patulin

[2] Mycotoxins highlighted in bold indicate a multiplex assay

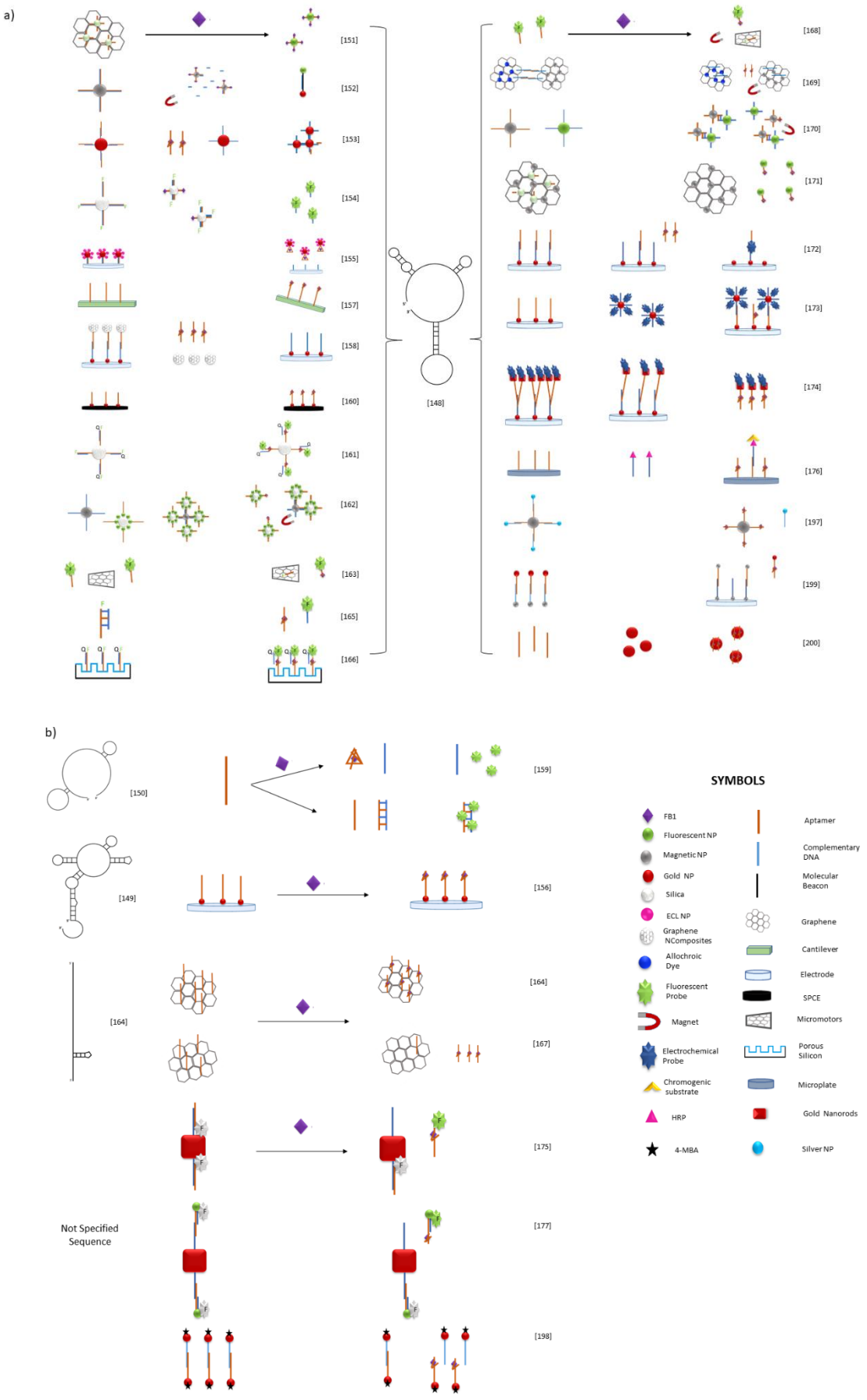

Figure 6. Schematic representation of the various mechanisms of aptamer-based biosensors with (a)the 96 nt aptamer and (b)other shorter or not specified sequences. (Abbreviations: **ECL:** Electrochemiluminescence; **HRP:** Horseradish peroxidase; **MBA:** Mercaptobenzoic acid, **NP:** Nanoparticle; **SPCMs:** Silica photonic crystal microspheres)

4.1 A 96-mer aptamer for fumonisin determination

The first aptamer specific for FB1 was reported by McKeague [148], after 18 SELEX rounds through negative selections with unmodified and modified (L-homocysteine, L-cysteine, L-methionine and L-glutamic acid) magnetic beads. From the six sequences initially studied, the sequence with the lowest G content (8 %) was selected due to its greatest binding affinity, confirmed by its low dissociation constant (Kd=100 nM). This sequence consisted in 60 random nucleotides (bold letters), surrounded by two primer binding sites: 5'-ATA CCA GCT TAT TCA ATT **AAT CGC ATT ACC TTA TAC CAG CTT ATT CAA TTA CGT CTG CAC ATA CCA GCT TAT TCA ATT** AGA TAG TAA GTG CAA TCT-3'.

4.1.1 Fluorescent detection

From all the biosensing designs applying the 96 nt aptamer, the most sensitive were those transduced into fluorescent [154, 166, 170] and electrochemical [172,173,174] signals. The first fluorescent method described the application of avidin-modified fluorescent nanoparticles and graphene oxide (GO), as donor/acceptor pair in Förster resonance energy transfer (FRET). A biotin modified aptamer was attached to upconversion fluorescent particles (UCNPs); under the presence of an increasing fumonisin concentration, the particles were not quenched by GO, thus exhibiting a linear increment on the fluorescence intensity [151]. The surface of reduced GO/platinum nanoparticles (PtNPs) and RGO/Ni/PtNPs micromotors were also used as a quencher of fluorescein amidine (FAM)-aptamers, with a direct increase on its fluorescence intensity produced by target biding [163, 168]. A similar procedure was proposed for the FRET-quenching effect between AuNP and UCNPs attached to a molecular beacon (MB), although the measured signal intensity was an indirect analysis of the fumonisin content. To this end, a biotinylated aptamer (linked to avidin modified magnetic particles), was hybridized with its complementary DNA, which was also able to hybridize and open the MB, thus forming a fluorescent double-stranded DNA arrangement [152].

In the most sensitive development with this long sequence, the functionalization of magnetic nanoparticles with aptamers and time-resolved fluorescent nanoparticles with complementary DNA, resulted in the formation of capture and signal probes, respectively. The DNA hybridization step derived to a magnetic/fluorescent biocomplex, whose magnetic separation at rising concentrations of FB reported a reduction in fluorescence intensity [170]. Similarly, amino modified aptamers hybridized with their fluorescein isothiocyanate (FTIC)- modified complementary DNA, were coupled to silica photonic crystal microspheres (SPCMs), with an inhibitory effect on the fluorescent signal caused by an increasing target concentration [154]. In fact, good sensitivity can be achieved with SPCM suspensions, when bound to a hybridized duplex structure formed by a black hole quencher (BHQ2)-labelled antiaptamer (quencher) and a NH_2(5')/Cy3(3') modified aptamer. An increasing FB1 concentration enlarged the separation between the dye and its corresponding quencher, promoting a higher fluorescent signal [161]. Moreover, the hybridization between a NH_2/Cy3 modified aptamer and its BHQ2-antiaptamer was examined when immobilized to a TiO_2 modified silicon wafer, where the increment of fluorescence was triggered by the addition of FB1 [166]. Unlike other techniques, a less sensitive electrochemiluminescent (ECL) assay resulted from AuNP modified with a thiolated aptamer and an iridium complex, when fixed to an Au electrode by a partial complementary DNA. As the AuNP/Ir complex enhanced the electrode conductivity, the addition of FB1 decreased its ECL signal [155]. A very sensitive aptasensor for FB1 combined the interaction of a biotinylated aptamer and its biotinylated complementary DNA, conjugated to magnetic and NaYF4:Ce/Tb nanoparticles respectively. The addition of the target mycotoxin produced a decrease on the complex formation, therefore a signal decrease on the resulting fluorescence [170].

4.1.2 Electrochemical detection

As already stated, electrochemical methods have also been applicable to sensitive FB1 aptasensors, and their precise completion can be enhanced by the addition of materials such as AuNP and graphene-thionine (GS-TH). Electrodes functionalized with AuNP are convenient for DNA attachment, and the complexity of its fabrication depends on the aptamer structure. For instance, the unmodified 96-mer molecule was docked to a AuNP modified glassy carbon electrode through a

thiolated capture DNA. A higher sensitivity was promoted by the addition of GS-TH, due to its competition against FB1 for binding the aptamer, which also generated a decrease in the redox peak [158]. Efforts for reducing the costs and increasing the capacity of aptasensors have focused on a combination of powerful electrochemical techniques with portable devices. A screen-printed carbon electrode (auxiliary, reference and working electrodes included) modified with polydimethylsiloxane was selected for the electrodeposition of AuNP, and further attachment of a thiolated aptamer. The coil to G-quadruplex conformational transition, supported by the presence of FB1, was applied to strengthen the electron transfer resistance, reflected as a reduction in the electrochemical impedance spectroscopy response [160]. While the previous methods were able to quantify FB1 in a ng/L scale, upcoming electrochemical assays are reaching limits of detection in the pg/L range.

Gold electrodes worked as ideal supports for combined DNA structures, as verified for double-stranded DNA (aptamer-cDNA). The incubation with different concentrations of FB1 in this assay left some free and hybridized cDNA that had to be subsequently washed with exonuclease I. The remaining double-stranded DNA interacted with methylene blue whose electrochemical signal reached a LOD of 0.00015 µg/L [172]. A Y-shaped hybridized structure was also conjugated on a gold electrode. This approach included a DNA sequence complementary on different segments to two aptamers and the addition of gold nanorods for signal enlargement related to concentrations of FB1 as low as 0.00026 µg/L [174]. Another technique in the pg/L scale (0.0005 µg/L) was designed on a glassy carbon electrode modified with molybdenum disulfide and gold nanoparticles for the attachment of aptamers and further immobilization with labelled cDNA, whose differential pulse voltammetry (DPV) decreased with the addition of FB1 [173].

4.1.3 Alternative and colorimetric detection

Alternative aptasensors comprised gold-modified microcantilevers, capable of containing thiolated aptamers, in which the differential deflection linearly increased with higher FB1 concentrations [157]. In a different novel method, Fe_3O_4@Au magnetic beads were also coupled with a thiolated complementary DNA, for the hybridization of amino-modified aptamers, conjugated with SiO_2@PbS hybrid spheres. An increasing concentration of FB1 produced a reduction on the number of hybridized labels, which after a magnetic separation were dissolved in acid for the square wave voltammetry of the remaining Pb^{2+} [162]. As already illustrated, magnetic beads promoted the easy separation of their unhybridized attached sequences, which was also reported for the fluorometric test of a FAM labelled complementary DNA displaced from its hybrid form with its corresponding aptamer, upon FB1 binding [165]. A similar approached was proposed with aptamer functionalized with magnetic beads, whose hybridization with cDNA-silver nanoparticles (AgNPs) was diminished by the presence of target, with further inductively coupled plasma mass spectrometry of Ag released as cDNA-AgNPs [197].

In order to reduce the complexity of the assays, three colorimetric methods have been proposed for the unmodified version of this aptamer. On the first system, gold nanoparticles were functionalized with either a thiolated short-strand (DNA1) complementary to the unmodified aptamer or a thiolated short-strand complementary to DNA1 (DNA2). The association of the aptamer and DNA1 was interrupted by the addition of FB1, which also permitted the hybridization of AuNP-DNA1 and AuNP-DNA2, causing aggregation and color shift from red to blue [153]. For the second approach, thymolphthalein was adsorbed on the surface of GO nanoparticles modified with a semi complementary DNA. The use of the unmodified 96-mer aptamer as a DNA linker, allowed the conjugation of the labelled GO with Fe_3O_4/GO, previously modified with a second semi complementary DNA. After target incubation, the Fe_3O_4/GO particles were magnetically removed, and a colorimetric detection was revealed by adjusting the pH of the remaining solution containing labelled GO [169]. Another colorimetric assay was proposed through the competition between a HRP-cDNA and FB1 for binding an aptamer immobilized on a streptavidin-coated microplate. Depending on the amount of FB1, a colorless TMB solution was catalyzed by the hybridized HRP-cDNA to obtain the blue oxTMB, whose yellow color was exposed by the stopping solution (sulfuric acid) [176]. A more complex colorimetric method was design through a glassy carbon electrode (GCE) modified with Fe_3O_4-cDNA-aptamer-AuNP at different degrees, due to dehybridization by FB1. Such sensing electrode was connected to a Pt wire through an electric bridge, where varying target concentrations

resulted in different GCE effective areas and current flow, reported as deposition of Prussian blue (PB) on an ITO electrode. This indirect electrochemical analysis was translated into a colorimetric signal by means of the smartphone detection of deposited PB at the ITO electrode, submerged in the reporting solution along with the Pt wire [199]. In contrast to previous reports, the sole application of the unmodified sequence (96 nt) was reported by our research group in an aptamer-FB1-AuNPs conjugate, stable to salt-induced aggregation at an increasing target concentration, under the presence of $MgCl_2$ [200].

4.2 Shorter sequences and minimers derived from the 96 nt aptamer

Five years after the dissemination of the first aptamer specific to FB1 [148], the same research group explored the affinity of minimers (truncated aptamers) from the initial 96 nt aptamer. The different structures included the whole sequence, and its subsequent chains created by preserving the 3' stem loop motif, removing the 3', 5', or both primer binding regions (PBR).

Larger melting temperatures from minimers containing the 3' region, suggested their role on the stability and complete formation of hairpins [150]. The same study compared the binding affinity through the calculation of the dissociation constant (Kd) by two assays: DNase I and magnetic beads. The DNase I assay indicated similar affinities between the minimer without the two PBR and the full-length oligonucleotide (Table 6); however, this method also carried considerable errors and denoted binding towards FB2. On the other hand, the magnetic beads confirmation assay proved the high affinity of minimers lacking the 3' and both PBR, as well as their overall upgraded binding, due to primary amine masking by the beads, suggesting a most favorable interaction with the tricarballylic acid regions [150]. A reduction on the sequence length might lead to the development of simpler, yet more sensitive biosensors. The interaction within the shorter 60 nt strand without PBR and its complementary DNA was tested under the presence of different concentrations of FB1, in which the rate of double-stranded DNA formation was identified with the fluorescent dye PicoGreen [159]. Regardless of the specificity issues presented by Frosts [150], the truncated sequence studied by Gui [159] was capable of discriminating ochratoxin A (OTA) aflatoxin B1 (AFB1), citrinin (CTN) and zearalenone (ZEN), while the specificity of the original long length aptamer was already confirmed for the null interaction with OTA, AFB1, AFB2, AFG1, AFG2, FB2, ZEN, L-cysteine, BSA, T-2 toxin and deoxynivalenol (DON)(Table 5). Still, even when this 60 nt aptamer-based method was correlated to a reduction on the assay and assay preparation times, its depicted LOD was higher than the values achieved with the full 96 nt sequence.

4.3 A novel oligonucleotide for the determination of FB1

Four years after the first reported sequence, a new aptamer selection was presented by using a library of single stranded DNA designed with 80 nt sequences, in which 40 random nucleotides (bold letters) were edged by 20 nt on each side. The SELEX process was executed with the aid of magnetic beads, and included negative (magnetic beads), positive (FB1 modified magnetic beads) and counter (free glycine, AFB1, AFB2, ZEN) selection rounds, which also served to confirm the aptamer selectivity. The selected aptamer: 5'-AGC AGC ACA GAG GTC AGA TG **C GAT CTG GAT ATT ATT TTT GAT ACC CCT TTG GGG AGA CAT** CCT ATG CGT GCT ACC GTG AA-3, showed a lower Kd (62 nM), hence a greater affinity to FB1 was expected for the development of more sensitive aptasensors than that with the 96 nt aptamers [149]; however, this was not the case and the aptasensors so far reported using this aptamer have not shown the expected superior sensitivity, which was also confirmed by its fewer applications.

After its introduction, the full-length thiolated version was docked on glassy carbon electrodes in order to enhance its electron transfer resistance, whose decrement was caused by the addition of the target mycotoxin [156]. This electrochemical arrangement derived in a sensitive method, with a similar LOD to previous electrochemical aptasensors for FB1 [157, 160]. Furthermore, a shorter version, consisting on its 40 random nucleotides, was casted on doped (B or N) and undoped graphene modified GCE, from which boron-doped graphene helped immobilize a higher amount of FB1, improving the impedimetric signal thus the sensitivity of the electrochemical sensor [164]. This 40 nt aptamer was also immobilized on graphene oxide nanocolloids (GONCs), causing a reduction on the electroactivity from the oxygen containing groups. The addition of FB1 prompted the full detachment

of the aptamer and the partial reestablishment of electroactivity, with potential for biosensing purposes and verified sensitivity under the presence of OTA and thrombin [167]. Although the latter corresponded to low assay and assay preparation times, both biosensors were not comparable to the applications with longer chains. Further research is needed to reveal the affinity mechanism for this aptamer to understand its sensitivity constrains and fully develop highly sensitive aptamer-based sensors.

4.4 Not specified sequences and alternative methods

Three studies published by the same research group did not specify the aptamers sequence for the detection of FB1. The first approach relied on the hybridization of Cy5.5-aptamer and its cDNA on gold nanorods, with a further measurement of their SERS (LOD: 0.0003 μg/L) and fluorescent (LOD:0.0005 μg/L) signals under the presence of the target mycotoxin [175]. The second work, which so far is the most sensitive aptasensor for FB1, was reported with a LOD of 0.000003 μg/L. In this arrangement, the inner filter effect between UCNPs and gold nanorods, both linked by a hybridized aptamer, was reduced by disrupting the biocomplex through target incubation and stimulating fluorescence under excitation (980 nm) [177]. The third biosensor combined the modification of AuNPs with aptamers and 4-mercaptobenzoic acid as a Raman reporter, whose signal was reduced after target incubation through dehybridization from a cDNA-AuNP-(4-MBA) complex, with an LOD of 0.00002 μg/L [198]. The effect of the electrochemical interaction between FB1 and fish sperm double-stranded DNA was examined on the impedimetric detection with a pencil graphite electrode, which provides a promising biosensing technique with other DNA structures apart from aptamers [178]. Nevertheless, the addition of five FB1 concentrations did not portray differentiated responses; therefore, more optimization would be ideal for the application of this type of non-specific sequences.

4.5 Multiplex detection

Aptasensors are not restricted to the sole determination of single mycotoxins, multiplex analysis can be accomplished with different arrays. Fluorescent [151] and magnetic [162, 197] nanoparticles, as well as their association [170,171], were applied for the multiple detection of FB1 and OTA. Moreover, photonic crystal microspheres were able to support double (FB1, OTA) and triple (FB1, OTA, AFB1) mycotoxin quantification [154, 161]. In a similar way to fluorescent particles, the application of fluorescent labels favored the establishment of optimum λ_{em} in combination with their specific reading methods (filters), for the detection of FB1 and OTA [163]. The specific allocation of a cy3 aptamer and its BHQ antiaptamer on TiO_2 modified silicon wafers, was also suitable for the linear quantification of multiple mycotoxins (OTA, AFB1, FB1), where the fluorescence increment was spotted on a defined area of a wafer surface [166]. The combination of two different fluorescent compounds with UCNPs induced two resolved responses under the presence of ZEN and FB1 [177], while the functionalization of UCNPs and AuNPs with aptamers along with aptamer labelling were exploited in the multiplex SERS and fluorescence detection of ZEN, OTA and FB1, through a triple hybridization with a cDNA-AuNPs complex [198]. Likewise, as previously mentioned, the combination of different allochroic dyes with magnetic and GO nanoparticles, was also convenient for the colorimetric detection of FB1, OTA, AFB1 and microcystin-LR [169].

Table 6 DNA sequences utilized for different aptasensor and their binding conditions[1]

Aptamer Modification	cDNA	Other	Binding Buffer	Incubation	Ref
5'-ATA CCA GCT TAT TCA ATT AAT CGC ATT ACC TTA TAC CAG CTT ATT CAA TTA CGT CTG CAC ATA CCA GCT TAT TCA ATT AGA TAG TAA GTG CAA TCT-3'					[148]
5′-Biotin-(CH2)6-	-	-	Tris-HCl buffer (10 mM containing 100 mM NaCl, pH 7.4)	37 °C Overnight (conjugation in BB) 37 °C, 2 h (Binding) 37 °C, 80 min (Incubation with GO)	[151]
5′-Biotin-(CH2)6-	5′-AAT TGA ATA AGC TGG-3	Molecular Beacon 5′-SH-(CH2)6-GCT CG CCA GCT TAT TCA ATT CGA GC-(CH2)6-H2N-3′	10 mM PBS	37 °C 12 h (immobilization on MNPs) 37 °C, 30 min (hibridization aptamer-cDNA) 37 °C, 30–40 min (incubation) 37 °C, 30 min (hibridization cDNA-MB)	[152]
None	5' -SH-AAT TGA ATA AGC TGG TA-3'	5'-SH TAC CAG CTT ATT CAA TT-3'	10 mM PB containing 1% SDS by mass pH 7.4 (DNA dilution) 500 Mm NaCl cDNA1 300 mM NaCl cDNA2 1 x PCR amplification buffer (Conjugate dilution) 20 mM NaCl + 10 mM PB	37 °C, shaking for 12 h (funtionalization) RT, overnight salt aging 95 °C, 5 min (hibridization cDNA1-cDNA2) Cool down RT	[153]
-(CH2)6-NH2-3′	5′-FITC-AAT TGA ATA AGC TGG TA-3′	-	TE solution (100 mM Tris-HCl + 10 mM EDTA) 5× saline sodium citrate (hibridization) 10mM Tris-HCl (pH 8.0), 120 mM NaCl, 20 mM CaCl2, 5 mM KCl, 20 mM $MgCl_2$ (binding)	4 °C, 12 h. (Immobilization on SPCMs in TE solution) 37 °C, 1 h. (blocking with 1B% BSA PBS) 37 °C, 2 h. (hibridization) 37 °C, 1 h (binding)	[154]
5′-SH-(CH2)6-	-SH-(CH2)6-AAT TGA ATA AGC TGG TAT	-	Methanol 50%	80 °C, 5 min (hibridization) Cooled to RT 37 °C, 2 h (binding)	[155]
5′-SH-(CH)6-	-	-	10 mM Tris–HCl, 100 mM NaCl, 100 mM TCEP, pH 7.4 (immobilization) 10 mM Tris–HCl, 100 mM NaCl pH 7.4. (binding)	3 h, 25 °C (Functionalization) 1 h, 25 °C with MCH (blocking) 10 min, 25 °C, (Incubation)	[157]
None	5'-SH-(CH2)6-AAT TGA ATA AGC TGG TA-3'	-	10 mM Tris-HCl buffer pH 7.4 (hibridization) PBS (pH 7.4). (binding)	24 h, RT (cDNA immobilization) 37 °C, 2 h. (hibridization) Room temperature, 25 min (binding)	[158]
5'-AAT CGC ATT ACC TTA TAC CAG CTT ATT CAA TTA CGT CTG CAC ATA CCA GCT TAT TCA ATT-3'	5'-AAT TGA ATA AGC TGG TAT GTG CAG ACG TAA TTG AAT AAG CTG GTA TAA GGT AAT GCG ATT-3'	-	10 mmol/L Tris, 120 mmol/L NaCl, 5 mmol/L KCl、20 mmol/L $CaCl_2$ (pH 8.5)	95 ℃, 5 min (denaturation) 10 min on ice 25 ℃, 20 min (Incubation) 25 ℃, 5 min (hibridization)	[159]
FB139t3: F- ATA CCA GCT TAT TCA ATT AAT CGC ATT ACC TTA TAC CAG CTT ATT CAA TTA CGT CTG CAC ATA CCA GCT TAT TCA ATT FB139t3-5: F- AAT CGC ATT ACC TTA TAC CAG CTT ATT CAA TTA CGT CTG CAC ATA CCA GCT TAT TCA ATT	-	-	100 mM NaCl, 20 mM Tris, 2 mM $MgCl_2$, 5 mM KCl, 1 mM $CaCl_2$, pH 7.6 (selection buffer)	DNase I assay: 30 min, RT (Incubation with FB1) Magnetic beads assay: 90 °C, 10 min (pre-heating) RT, 30 min RT, 60 min (Incubation)	[150]
5′-SH-(CH2)6-	-	-	Aptamer stock: 50 mM Tris-HCl buffer (ph 7.4, 0.1M NaCl, 0.2M KCl, 5 mM $MgCl_2$ and 1 mM EDTA) Activation Buffer: 50 mM Tris-HCl with 100 mM TCEP Activated aptamer: 50 mM Tris-HCl pH 7.4 with 1.0 mM EDTA) PBS 0.1M, pH 7.4 Binding buffer: TE buffer containing 0.1 M NaCl, 0.2 M KCl, and 5.0 mM $MgCl_2$	Room temperature, 1 h (activation) 6 h and 4 °C (SPCE modification with activated aptamer) 1 h, RT (Blocking with MCH) Room temperature, 30 min h (binding)	[160]
5′-NH2-(CH2)6-reverse sequence-Cy3-*3′	5′-BHQ2-TAT GGT CGA ATA AGT TAA-3′	-	Binding buffer: Tris-HCl, 0.01 M, pH 8.0, NaCl 120 mM, $CaCl_2$ 20 mM, KCl, 5 mM, $MgCl_2$ 20 mM	60 min and 37 °C (hibridization) Room Temperature 12 h (Immobilization on microspheres) 90 min and 45 °C (binding)	[161]
–NH2–3′	5′-TTG AAT AAG CTG GTA TAA GGT AAT GCG ATT AAT TGA ATA AGC TGG TAT–SH–3′	-	10 mM Tris-HCl, 1 mM EDC, 1 mM NHS (aptamer conjugation) 10 mM Tris-HCl with 100 mM TCEP (cDNA activation)	37 °C, overnight (aptamer conjugation) 37 °C, 1 h. (cDNA activation) 37 °C, 30 min (cDNA incubation with MBs) RT, 1 h (blocking with MCH) 37 °C, 2 h. (hibridization) 37 °C, 1 h (binding)	[162]

5′-FAM-		-	Tris-HCl pH 7.5; 10 mM PBST: 100 mM PBS (pH 7.5) with 0.01% Tween (Aptamer dilution)	25 ℃, 15 min (Incubation)	[163]
None	FAM- AATAAGCTGGTATGT	-	20 mM Tris, 0.1 M NaCl, 2 mM $MgCl_2$, 5 mM KCl, 1 mM $CaCl_2$ pH 7.6 (Binding buffer)	95 ℃, 5 min (Heating) 5 min on ice 37 °C, 1 h. (hibridization)	[165]
5′-NH2−(CH2)6- reverse sequence-Cy3-3’	5′-BHQ2-TAT GGT CGA ATA AGT TAA-3′	-	Binding buffer: Tris-HCl 10 mM (pH 8.0), NaCl 120 mM, $CaCl_2$ 20 mM, KCl 5 mM,$MgCl_2$ 20 mM)	88 ℃, 5 min (Heating in BB) 25 ℃, 2 h (aptamer-antiaptamer mixture and incubation) 37 ℃, 12 h (hibridization-immobilization) 37 ℃, 12 h (Binding)	[166]
5′-FAM-	-	-	10 mM Tris-HCl pH 7.5 (aptamer reconstitution/ incubation) SDS 1% v/v (aptamer capture) PBS 100 mM pH 7.5 with Milli-Q water and 0.01% of Tween (PBS-T) (Aptamer dilution)	25 ℃, 15 min (Incubation) RT, 2 min (Aptamer capture)	[168]
None	5’-GTG TGT GTG TGT GTG TGT GTG TGT GTG TGT AGA TTG CAC TTA CTA TCT AAT TGA ATA AGC TGG TAT GTG CAG ACG TAA-3’	5’-TTG AAT AAG CTG GTA TAA GGT AAT GCG ATT AAT TGA ATA AGC TGG TAT GTG TGT GTG TGT GTG TGT GTG TGT-3’	PBS, (Na_2HPO_4−NaH_2PO_4, 0.1 M)	RT, 2 h (DNA1 binding on GO) RT, 24 h (DNA2 immobilization on Fe3O4/GO) RT, 12 h (hibridization) 37 ℃, 1.5 h (Incubation)	[169]
5′-biotin-(CH2)6-	5′-biotin-(CH2)6-TCT AAT TGA ATA AGC TGG TAT GTG CAG ACG-3′	-	PBS (10 mM Na_2HPO_4, 137 mM NaCl, 2.7 mM KCl, 2 mM KH_2PO_4, pH 7.4)	37 ℃, 1 h (Incubation)	[170]
–NH2–3′	-	-	PBS 0.1M (pH 7.4)	RT, overnight (bio-probe) RT, overnight (Immobilization) 37 ℃, 1 h (Incubation)	[171]
None	5′-SH-GAG GGG TGG GCG GGA GGG AGA TTG CAC GGA CTA TCT AAT TGA ATA AGC-3′		Tris–HCl buffer (containing 0.05 M Tris, 0.2 M NaCl and 0.001 M EDTA)	37 ℃ (cDNA Immobilization) 37 ℃, 2 h (hibridization) 37 ℃, 10 min (Incubation FB1) 37 ℃, 30 min (Incubation Exo-I)	[172]
5′-SH-(CH2)6	5′-SH-(CH2)6-AATTGAATAAGCTGG 3′		TE Buffer (solutions, washing) PBS (0.1 M, ph 6.0)	95 ℃, 5 min (Heating) RT 1h (Cooling) 37 ℃, 2 h (Ap conjugation to electrode) 37 ℃, 2 h (hibridization) 15 min (Incubation)	[173]
5′-SH-	5′-SH-GAG GGG TGG AGA TTG CAC TTA CTA TCT AAT TGA GGG GGG TGT CCG ATG CTC-3′		50 mM Tris-HCl	2 h (Conjugation to AuNRs) 37 ℃ , 2 h (cDNA Immobilization on electrode) 37 ℃, 2 h (hibridization) 37 ℃, 10 min (Incubation)	[174]
5’-biotin	5’-biotin- AGA TTG CAC TTA CTA TCT AAT TGA ATA AGC TGG TAT GTG CAG ACG TAA TTG AAT AAG CTG GTA TAA GGT AAT GCG ATT AAT TGA ATA AGC TGG TAT -30.		PBS buffer (10 mmol/L Na_2HPO_4, 2 mmol/L KH_2PO_4, 2.7 mmol/L KCl, 137 mmol/L NaCl, pH 7.4) PBS-T (Washing)	37 ℃, 30 min (Immobilization) 25 ℃, 60 min (Immobilization)	[176]
5’-biotin	5’-biotin-GAT AGG AGT CGT GTG GGA TAG TGT GGG AGA TTG CAC TTA CTA TCT AAT TGA ATA AGC TGG TAT GTG CAG ACG TAA-3’		Tris-HCl buffer 20 mmol/L with 0.5 mol/L NaCl,1 mmol/L EDTA (Washing) 20 mM Tris-HCl pH 7.4 (Dissolving/Target Incubation) 100 mM Tris-HCl pH 7.4 (Re-dispersion)	37 ℃, 120 min (Functionalization of magnetic beads) 37 ℃, 90 min (Labelling of Ag NPs) 37 ℃, 120 min (Hibridization) 37 ℃, 120 min (Target Incubation)	[197]
5′-SH-C6-	5-NH2-C6-AAT TGA ATA AGC TGG TA-3’	5-SH-C6-GTTGGTGAGTCCAACCACACCA-3’ (Control DNA)	PBS, pH 7.4, 1× (Washing, redispersion, AuNP stability) Tris-HCl buffer 0.01 M, pH 7.4 (Hibridization, target incubation)	37 ℃, 120 min (Functionalization of Fe_3O_4) 37 ℃, 30 min (Hibridization) 37 ℃, 30 min (Target Incubation)	[199]
5’-AGC AGC ACA GAG GTC AGA TGC GAT CTG GAT ATT ATT TTT GAT ACC CCT TTG GGG AGA CAT CCT ATG CGT GCT ACC GTG AA-3’					[149]
5′-SH-(CH2)6-	-	-	pH 7.4, 100 mM NaCl, 20 mM Tris–HCl, 2 mM $MgCl_2$, 5 mM KCl, 1 mM CaCl2	37 °C, 6 h (electrode modification) 94 °C, 5 min followed by 15 min cooling with ice (folding) Room temperature, 30 min (binding)	[156]
5’-C GAT CTG GAT ATT ATT TTT GAT ACC CCT TTG GGG AGA CAT- 3’	-	-	PBS pH 7.0 (aptamer solution) Tris buffer pH 8.2(FB1 solution)	60 °C, 15 min (aptamer dropcasting) 37 °C, 30 min (Incubation)	[164]
5’-C GAT CTG GAT ATT ATT TTT GAT ACC CCT TTG GGG AGA CAT- 3’	-	-	Aptamer dilution: PBS (10 mM Na_2HPO_4; 100 mM NaCl; pH 7.2) FB1 dilution: Tris (25 mM Tris; 300 mM NaCl; pH 8.2).	60 ℃, 10 min (cast on GONC) 25 ℃, 5 min (washing in PBS) 37 ℃, 1 h (Incubation)	[167]
NOT SPECIFIED SEQUENCES					

Cy5.5	cDNA	-	10 mM Tris-HCl, 100 mM NaCl, 1 mM EDTA, pH 8.0 (hibridization buffer) 50 mM TE buffer pH 7.4 (Extract adjustment)	37 ℃, 1 h (Hibridization) 37 ℃, 45 min (Incubation/Hibridization)	[175]
None	cDNA1	cDNA2	PBS containing 0.9% NaCl (Hybridization buffer)	RT, 12 h (cDNA2 attachment on AuNR) RT, 12 h (UCNPs funtionalization with aptamers) RT, 12 h (Addition of cDNA1 to aptamer-UCNPs) 60 ℃, 50 min (Hibridization with cDNA2-AuNR) 37 ℃, 50 min (Cooling) 37 ℃, 50 min (Incubation)	[177]
NS	cDNA		Hybridization buffer (not specified) PBS buffer(redispersion) 50 mM TE buffer pH 7.4 (pH adjustement)	37 ℃, 12 h (Hibridization) 37 ℃, 2 h (Target Incubation)	[198]
None	-	-	$MgCl_2$ 1mM	37 ℃, 30 min (Target Incubation) RT, 60 min (Functionalization of AuNP)	[200]

[1] Abbreviations: **AuNRs:** Gold nanorods; **BB:** Binding buffer; **BSA:** Bovine serum albumin; **cDNA:** Complementary DNA; **GO:** Graphene oxide; **GONC:** Graphene oxide nanocolloids; **MCH:** 6-mercapto-1-hexanol; **NS:** Not specified; **RT:** Room temperature; **SPCE:** Screen-printed carbon electrode; **SPCM:** Silica photonic crystal microsphere; **UCNPs:** Upconversion fluorescent nanoparticles

Recent improved electrochemical methods also allowed multiplex analysis, as in the case of glassy carbon electrodes modified with enhancers of electron mobility such as MoS_2 and AuNP. These were utilized for the simultaneous quantification of FB1 and ZEN produced by the different reduction peaks from FC6S and thionine, respectively, which functioned as labels for cDNA when simultaneously immobilized on colloidal gold [173]. Likewise, gold electrodes modified with a Y-shaped DNA conformation were efficient for detecting OTA and FB1 due to immobilization of thiolated thionine and ferrocene on gold nanorods, which in addition of enhanced electron transfer, exhibited distinctive peak currents [174].

4.6 Aptamer folding and aptasensing comparison

As presented in Figure 7, the 96 nt and 80 nt aptamers [148, 149] displayed a more complex structure, mostly expressed by the formation of multiple stem loops, in contrast with the simple folded organization of the reduced aptamers and minimers [150, 167]. The final structure, predicted in Mfold, relied on the folding temperature, commonly varying from ice to room temperature, along with the ions present in the buffer (Mg^{+2}, Na^{+}). On that note, ongoing attempts by our research group to develop a AuNP-based colorimetric assay unveiled the role of different binding buffers on the final assay specificity [200]. Unlike previous aptasensors [164, 167], assays with the 40 nt aptamer under the presence of Tris HCl denoted lack of specificity when OTA was included [200].

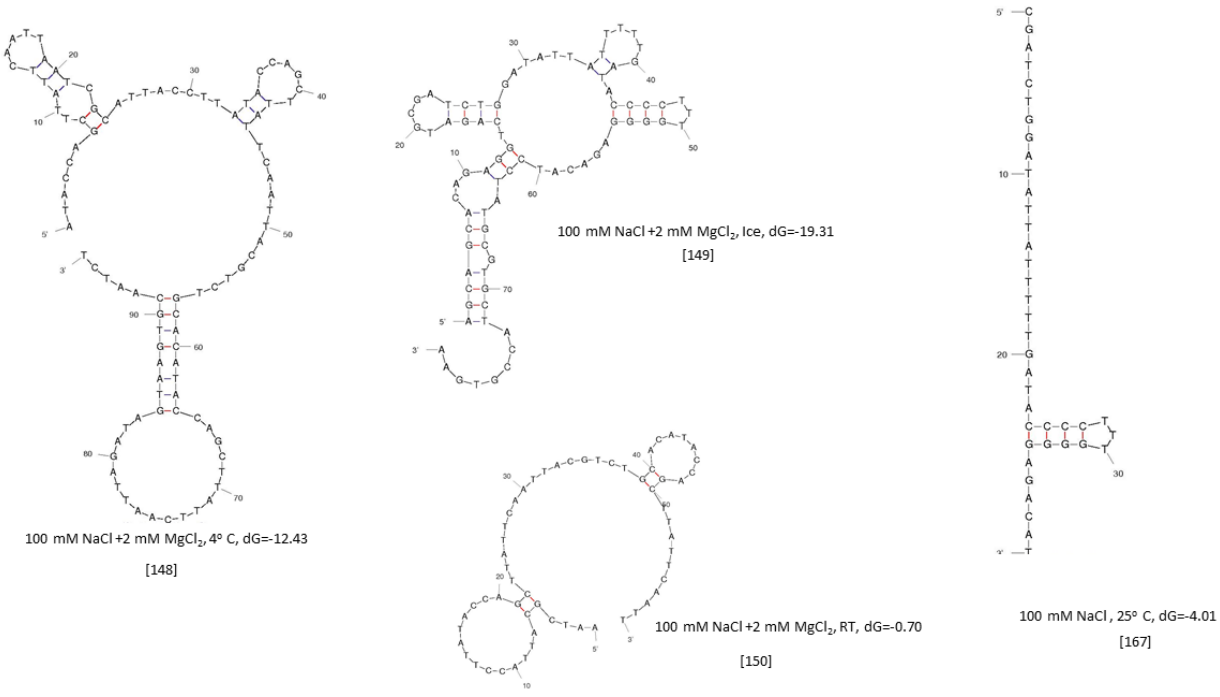

Figure 7. Aptamer folding forms obtained in Mfold at the specified conditions

A PCA specific to all the aptamer-based biosensors for FB1, is indicated in Figure 8, by using LODmax, ATmax and APmax of 100 μg/L [169], 720 minutes [166] and 12900 minutes [151], respectively. As already noted, assays with a hybridized 96 nt aptamer were mainly correlated to the lowest LOD's through fluorescent [151, 152, 161, 166, 170], chemiluminescent [155], optical [169] and MS [197] detections, along with fluorescent and SERS signals obtained from a non-specified hybridized aptamer [177, 198]. On the other hand, the shortest assay times were correlated to applications with the 96 nt aptamer in its end-modified [157, 160, 163, 168] and hybridized forms [158, 165, 173, 174], as well as electrochemical designs with some shorter sequences including a thiol modified 80 nt aptamer[156] and an unmodified 40 nt [164] sequence. Likewise, the assay preparation time showed high correlation to 60 nt fluorescent [159], 40 nt electrochemical [167], and 96 nt

colorimetric [200] aptasensors. Nevertheless, as already stated, the high correlation of the 96 nt aptamer with a high sensitivity (low LODs) in combination with its convenient specificity, were relevant for the existence of more biosensors based on this long length sequence. In addition, more robust techniques might be ideal for increasing the sensitivity of aptasensors. For instance, the analysis of the signals from the unique complex produced by the incubation of the 96 nt aptamer, FB1 and AuNP in particular buffer conditions ($MgCl_2$ 1mM), can be translated to LODs as low as 3 µg/L levels (analysis of spectral scan) with a refining to 56 pg/L, when employing techniques such as asymmetric flow field-flow fractionation (AF4) for resolving those complexes [200]. It is worth noting that no paper-based biosensor has so far been developed with any of the aptamers, whose application could reduce the cost and extend the applicability of such sensitive conformations.

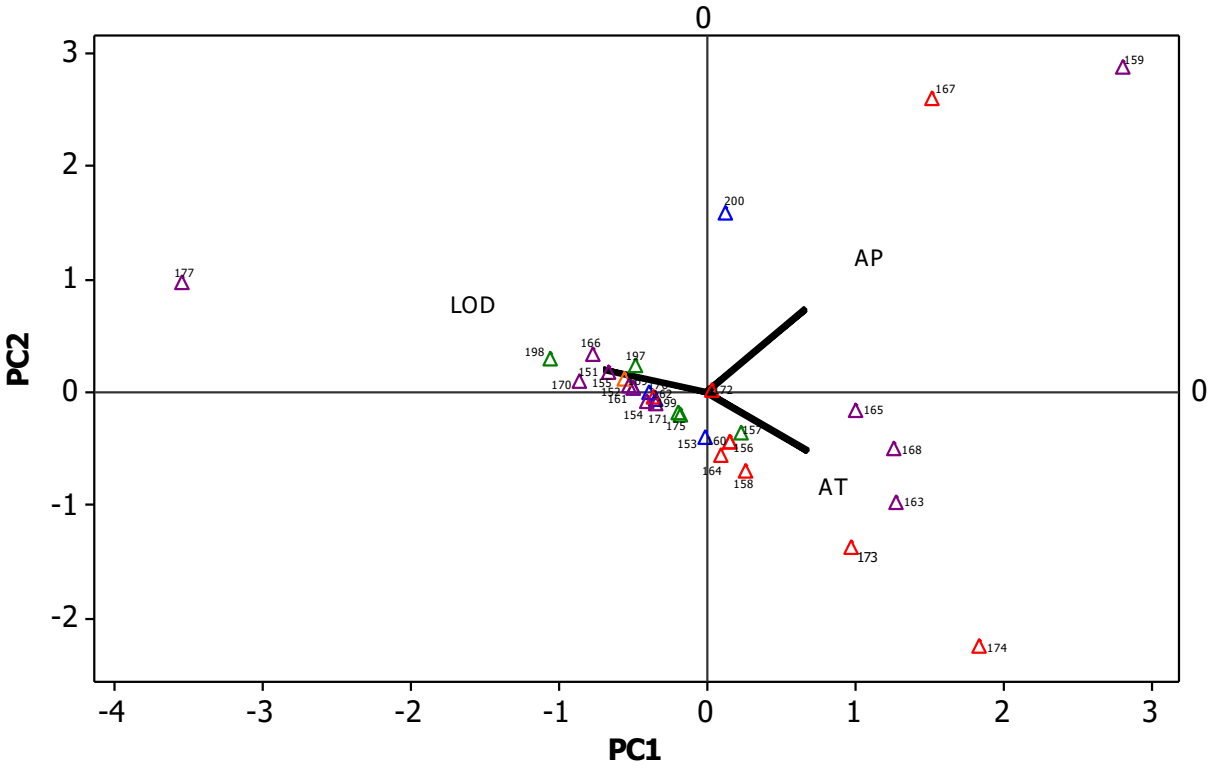

Figure 8. Principle component analysis for the correlation of all the reported aptasensors for optical (Δ), fluorescent (Δ), chemiluminescent (Δ), electrochemical (Δ), and other signals (Δ). The numbers correspond to the correlated references from Table 5.

5 Conclusions

The use of aptamers for the quantification of fumonisin B1 is at the central focus in the field of biosensors with many areas of opportunity, on account of their relatively recent dissemination and the few strands already reported. Even when sensitive, aptasensors featured similar or lower detections limits than well-established immunosensing techniques, LC-MS assays and Raman-based methods, the recent application of MIPS has redirected the attention on the improvement of the LODs from aptamer-based biosensors. Additionally, despite the diversity of approaches performed with the two selected aptamers and their shortened forms, to date around 95% of all the aptasensors have been proposed as bulk experiments. Hence, there is considerable room of opportunity for the exploration of different supports, ideally paper matrices for the refinement of on-site testing. Additionally, reducing the extraction steps is a desirable quality for quick analysis of samples in remote areas.

Thus far, the specificity of the aptamers utilized for FB1 quantification has been confirmed against up to 19 different molecules, and in multiplex detections of up to 4 targets, while their limits of detection confirmed the feasibility of addressing contamination levels under the regulated limits. It is important to understand and uncover the role of the selected support, and binding conditions (binding buffer, temperature, time) on the selectivity and affinity of the resulting biosensor. Despite all

the advances regarding aptamers, more efforts are necessary to obtain shorter strands with high affinity towards FB1 or novel targets, so the final sensing method can be simplified, yet be effective.

Acknowledgments: V.A. Miron-Merida acknowledges Mexico's National Council of Science and Technology (CONACyT) for their support in his Postgraduate Studies through and Academic Scholarship.

Conflicts of Interest: The authors declare no conflict of interest.

References

1. Marin, S., Ramos, A.J.; Cano-Sancho, G.; Sanchis, V. Mycotoxins: Occurrence, toxicology, and exposure assessment. *Food Chem Toxicol*, **2013**, *60*, pp.218-237.
2. Karlovsky, P.; Shman, M.; Berthiller, F.; De Meester, J.; Eisenbrand, G.; Perrin, I.; Oswald, I.P.; Speijers, G.; Chiodini, A.; Recker, T.; Dussort, P. Impact of food processing and detoxification treatments on mycotoxin contamination. *Mycotoxin Res* **2016**, *32(4)*, pp.179-205.
3. Bennett, J.W.; Klich, M. Mycotoxins. *Clin Microbiol Rev* **2003**, *16(3)*, pp.497-516.
4. European Commission. 2018. RASFF portal. Available online: https://ec.europa.eu/food/safety/rasff_en (Accessed on 07 April 2020)
5. Lamprecht, S.C.; Marasas, W.F.O.; Alberts, J.F.; Cawood, M.E.; Gelderblom, W.C.A.; Shephard, G.S.; Thiel, P.G.; Calitz, F.J. Phytotoxicity of fumonisins and TA-toxin to corn and tomato. *Phytopathology* **1994**, *84(4)*, pp.383-391.
6. Rheeder, J.P.; Marasas, W.F.O.; Vismer, H.F. Production of fumonisin analogs by *Fusarium* species. *Appl Environ Microbiol* **2002,** *68(5)*, pp.2101-2105.
7. Gelderblom, W.C.A.; Jaskiewicz, K.; Marasas, W.F.O.; Thiel, P.G.; Horak, R.M.; Vleggar, R.; Kriek, N.P.J. Fumonisins- Novel mycotoxins with cancer-promoting activity produced by *Fusarium moniliforme*. *Appl Environ Microbiol* **1988**, *54(7)*, pp.1806-1811.
8. Abbas, H.K.; Vesonder, R.F.; Boyette, C.D.; Hoagland, R.E.; Krick, T. Production of fumonisins by *Fusarium moniliforme* cultures isolated from jimsonweed in Mississippi. *J Phytopathol* **1992**, *136(3)*, pp.199-203.
9. Bezuidenhout, S.C.; Gelderblom, W.C.A.; Gorst-Allman, C.P.; Horak, R.M.; Marasas, W.F.O.; Spiteller, G.; Vleggaar, R. Structure elucidation of the fumonisins, mycotoxins from *Fusarium moniliforme*. *J Chem Soc D* **1988**, *0(11)*, pp.743-745.
10. Branham, B.E.; Plattner, R.D. Isolation and characterization of a new fumonisin from liquid cultures of *Fusarium moniliforme*. *J Nat Prod* **1993**, *56(9)*, pp.1630-1633.
11. Abbas, H.K.; Riley, R.T. The presence and phytotoxicity of fumonisins and AAL-toxin in Alternaria alternate. *Toxicon* **1995**, *34(1)*, pp.133-136.
12. Frisvad, J.C.; Smedsgaard, J.; Samson, R.A.; Larsen, T.O.; Thrane, U. Fumonisin B_2 production by *Aspergillus niger*. *J Agric Food Chem* **2007**, *55(23)*, pp.9727-9732.
13. Månsson, M.; Klejnstrup, M.L.; Phipps, R.K.; Nielsen, K.F.; Frisvad, J.C.; Gotfredsen, C.H.; Larsen, T.O. Isolation and NMR characterization of Fumonisin B_2 and a new fumonisin B_6 from *Aspergillus niger*. *J Agric Food Chem* **2010**, *58(2)*, pp.949-953.
14. Mogensen, J.M.; Møller, K.A.; Freiesleben, P.; Labuda, R.; Varga, E.; Sulyok, M.; Kubatova, A.; Thrane, U.; Andersen, B.; Nielsen, K.F. Production of fumonisins B_2 and B_4 in *Tolypocladium* species. *J Ind Microbiol Biotechnol* **2011**, *38(9)*, pp.1329-1335.
15. Ostry, V.; Malir, F.; Toman, J.; Grosse, Y. Mycotoxins as human carcinogens-the *IARC Monographs* classification. *Mycotoxin Res* ***2017***, *33(1)*, pp.65-73.

16. Gutleb, A.C.; Morrison, E.; Murk, A.J. Cytotoxicity assays for mycotoxins produced by *Fusarium* strains: a review. *Environ Toxicol Pharmacol* **2002**, *11(3-4)*, pp.309-320.
17. Riley, R.T.; Merrill, A.H. Ceramide synthase inhibition by fumonisins: a perfect storm of perturbed sphingolipid metabolism, signaling, and disease. *J Lipid Res* **2019**, *60(7)*, pp.1183-1189.
18. Régnier, M.; Polizzi, A.; Lukowicz, C.; Smati, S.; Lasserre, F.; Lippi, Y.; Naylies, C.; Laffitte. J.; Bétoulières, C.; Montagner, A.; Ducheix, S.; Gourbeyre, P.; Ellero-Simatos, S.; Menard, S.; Bertrand-Michel, J.; Al Saati, T.; Lobaccaro, J.M.; Burger, H.M.; Gelderblom, W.C.; Guillou, H.; Oswald, I.P.; Loiseau, N. The protective role of liver X receptor (LXR) during fumonisin B1-induced hepatotoxicity. *Arch Toxicol* **2019**, *93*, pp. 505-517.
19. Liu, X.; Fan, L.; Yin, S.; Chen, H.; Hu, H. Molecular mechanisms of fumonisin B1-induced toxicities and its applications in the mechanism-based interventions. *Toxicon* **2019**, *167*, pp.1-5.
20. Yuan, Q.; Jiang, Y.; Fan, Y.; Ma, Y.; Lei, H.; Su, J. Fumonisin B1 induces oxidative stress and breaks barrier functions in pig iliac endothelium cells. Toxins **2019**, *11*, pp.387.
21. Sharma, S.K.; Sharma, S.P.; Miller, D.; Parel. J.M.A.; Leblanc, R.M. Interfacial behavior of fumonisin B1 toxin and its degradation on the membrane. *Langmuir* **2019**, *35(7)*, pp.2814-2820.
22. Marasas, W.F.O.; Jaskiewicz, K.; Venter, F.S.; Van Schalkwyk, D.J. *Fusarium moniliforme* contamination of maize in oesophageal cancer areas in Transkei. *S Afr Med J* **1988**, *74(3)*, pp.110-114.
23. Yoshizawa, T.; Yamashita, A.; Luo, Y. Fumonisin occurrence in corn from high- and low-risk areas for human esophageal cancer in China. *Appl Environ Microbiol* **1994**, *60(5)*, pp.1626-1629.
24. Missmer, S.A.; Suarez, L.; Felkner, M.; Wang, E.; Merrll Jr.; A. H.; Rothman, K.J.; Hendricks, K.A. Exposure to fumonisins and the occurrence of neural tube defects along the Texas-Mexico border. *Environ Health Perspect* **2006**, *114(2)*, pp.237-241.
25. Magoha, H.; De Meulenaer, B.; Kimanya, M.; Hipolite, C.L.; Kolsteren, P. Fumonisin B1 contamination in breast milk and its exposure in infants under 6 months of age in Rombo, Nothern Tanzania. *Food Chem Toxicol* **2014**, *74*, 112-116.
26. Riley, R.T.; Torres, O.; Matute. J.; Gregory, S.G.; Ashley-Koch, A.E.; Showker, J.L.; Mitchell, T.; Voss, K.A.; Maddox, J.R.; Gelineau-van Waes, J.B. Evidence for fumonisin inhibition of ceramide synthase in humans consuming maize-based foods and living in high exposure communities in Guatemala. *Mol Nutr Food Res* **2015**, *59(11)*, pp.2209-2224.
27. Torres, O.; Matute, J.; Gelineau-van Waes, J.; Maddox, J.R.; Gregory, S.G.; Ashley-Koch, A.; Showker, J.l.; Zitomer, N.C.; Voss, K.A.; Riley, R.T. Urinary fumonisin B1 and estimated fumonisin intake in women from high- and low- exposure communities in Guatemala. *Mol Nutr Food Res* **2014**, *58(5)*, pp.973-983.
28. Chen, C.; Mitchell, N.J.; Gratz, J.; Houpt, E.R.; Gong, Y.; Egner, P.A.; Groopman, J.D.; Riley, R.T.; Showker, J.L.; Svensen, E.; Mduma, E.R.; Patil, C.L.; Wu, F. Exposure to aflatoxin and fumonisin in children at risk for growth impairment in rural Tanzania. *Environ Int* **2018**, *115*, pp.29-37.
29. Food and Agriculture Organization of the United Nations. 2004. *Worldwide regulations for mycotoxins in food and feed in 2003* (31 December 2003). Available online: http://www.fao.org/docrep/007/y5499e/y5499e00.htm (Accessed on 31 October 2017)
30. Udomkun, P.; Wiredu, A.N.; Nagle, M.; Bandyopadhyay, R.; Müller, J.; Vanlauwe, B. Mycotoxins in Sub-Saharan Africa: Present situation, socio-economic impact, awareness, and outlook. *Food Control* **2017**, *72(A)*, pp.110-122.

31. Bartók, T.; Szécsi, A.; Szekeres, A.; Mesterházy, A.; Bartók, M. Detection of new fumonisin mycotoxins and fumonisin-like compounds by reversed-phase high-performance liquid chromatography/electrospray ionization ion trap mass spectrometry. *Rapid Commun Mass Spectrom* **2006**, *20(16)*, pp.2447-2462.
32. Savi, G.D.; Piacentini, K.C.; Marchi, D.; Scussel, V.M. Fumonisins B_1 and B_2 in the corn-milling process and corn-based products, and evaluation of estimated daily intake. *Food Addit Contam: Part A* **2016**, *33(2)*, pp.339-345.
33. Yamagishi, D.; Akamatsu, H.; Otani, H.; Kodama, M. Pathological evaluation of host-specific AAL-toxins and fumonisin mycotoxins produced by *Alternaria* and *Fusarium* species. *J Gen Plant Pathol* **2006**, *72(5)*, pp.323-327.
34. Noonim, P.; Mahakarnchanakul, W.; Nielsen, K.F.; Frisvad, J.C.; Samson, R.A. Fumonisin B_2 production by *Aspergillus niger* in Thai coffee beans. *Food Addit Contam: Part A* **2009**, *26(1)*, pp.94-100.
35. Varga, J.; Kocsubé, S.; Suri, K.; Szigeti, G.; Szekeres, A.; Varga, M.; Tóth, B.; Bartók, T. Fumonisin contamination and fumonisin producing black Aspergilli in dried vine fruits of different origin. *Int J Food Microbiol* **2010**, *143(3)*, pp.143-149.
36. Hossain, S.M.; Luckham, R.E.; Smith, A.M.; Lebert, J.M.; Davies, L.M.; Pelton, R.H.; Filipe, C.; Brennan, J.D. Development of a bioactive paper sensor for detection of neurotoxins using piezoelectric inkjet printing of sol-gel-derived bioinks. *Anal Chem* **2009**, *81(13)*, pp.5474–5483.
37. Lee, S.; Kim, G.; Moon, J. Performance improvement of the one-dot lateral flow immunoassay for Aflatoxin B1 by using a smartphone-based reading system. *Sensors* **2013**, *13(4)*, pp.5109-5116.
38. Ueno, Y.; Iijima, K.; Wang, S.-D.; Sugiura, Y.; Sekijima, M.; Tanaka, T.; Chen, C.; Yu, S.-Z. Fumonisins as a possible contributory risk factor for primary liver cancer: a 3-year study of corn harvested in Haimen, China, by HPLC and ELISA. *Food Chem Toxicol* **1997**, *35(12)*, pp.1143-1150.
39. Campa, R.; Miller, D.; Hendricks, K. Fumonisin in tortillas produced in small-scale facilities and effect of traditional masa production methods on this mycotoxin. *J Agric Food Chem* **2004**, *52*, pp.4432-4437.
40. Gong, Y.Y.; Torres-Sanchez, L.; Lopez-Carrillo, L.; He Peng, J.; Sutcliffe, A.E.; White, K.L.; Humpf, H-U.; Turner, P.C.; Wild, C.P. Association between tortilla consumption and human urinary fumonisin B1 levels in a Mexican population. *Cancer Epidemiol Biomarkers Prev,* **2008**, *17(3)*, pp.688-694.
41. Dall'Asta, C.; Mangia, M.; Berthiller, F.; Molinelli, A.; Sulyok, M.; Schuhmacher, R.; Krska, R.; Galaverna, G.; Dossena, A.; Marchello, R. Difficulties in fumonisin determination: the issue of hidden fumonisins. *Anal BioanalChem* **2009**, *395(5)*, pp.1335-1345.
42. Ghali, R.; Ghorbel, H.; Hedilli, A. Fumonisin determination in Tunisian foods and feeds. ELISA and HPLC methods comparison. *J Agric Food Chem* **2009**, *57(9)*, pp.3955-3960.
43. Gazzotti, T.; Lugoboni, B.; Zironi, E.; Barbarossa, A.; Serraino, A.; Pagliuca, G. Determination of fumonisin B1 in bovine milk by LC-MS/MS. *Food Control* **2009**, *20(12)*, pp.1171-1174.
44. Silva, L.J.G.; Pena, A.; Lino, C.M.; Fernández, M.F.; Mañes, J. Fumonisin determination in urine by LC-MS-MS. *Anal BioanalChem* **2010**, *396(2)*, pp.809-816.
45. Tansakul, N.; Jala, P.; Laopiem, S.; Tangmunkhong, P.; Limsuwan, S. Co-occurrence of five Fusarium toxins in corn-dried distiller´s grains with solubles in Thailand and comparison of ELISA and LC-MS/MS for fumonisin analysis. *Mycotoxin Res* **2013**, *29(4)*, pp.255.260.
46. Petrarca, M.H.; Rodrigues, M.I.; Rossi, E.A.; De Sylos, C.M. Optimisation of a simple preparation method for the determinations of fumonisin B1 in rice. *Food Chem* **2014**, *158*, pp.270-277.

47. Bordin, K.; Rottinghaus, G.E.; Landers, B.R.; Ledoux, D.R.; Kobashigawa, E.; Corassin, C.H.; Oliveira, C.A.F. Evaluation of fumonisin exposure by determination of fumonisin B1 in human hair and in Brazilian corn products. *Food Control* **2015**, *53*, pp.67-71.
48. Liu, H.; Luo, J.; Kong, W.; Liu, Q.; Hu, Y.; Yang, M. UFLC-ESI-MS/MS analysis of multiple mycotoxins in medicinal and edible *Areca catechu*. *Chemosphere* **2016**, *150*, pp.176-183.
49. Li, M.; Kong, W.; Li, Y.; Liu, H.; Liu, Q.; Dou, X.; Ou-yang, Z.; Yang, M. High-throughput determination of multi-mycotoxins in Chinese yam and related products by ultra fast liquid chromatography coupled with tandem mass spectrometry after one-step extraction. *J Chromatogr B* **2016**, *1022*, pp. 118-125.
50. Xing, Y.; Meng, W.; Sun, W.; Li, D.; Yu, Z.; Tong, L.; Zhao, Y. Simultaneous qualitative and quantitative analysis of 21 mycotoxins in Radix Paeoniae Alba by ultra-high performance liquid chromatography quadrupole linear ion trap mass spectrometry and QuEChERS for sample preparation. *J Chromatogr B* **2016**, *1031*, pp.202-213.
51. Danezis, G.P.; Anagnostopoulos, C.J.; Liapis, K.; Koupparis, M.A. Multi-residue analysis of pesticides, plant hormones, veterinary drugs and mycotoxins using HILIC chromatography e MS/MS in various food matrices. *Anal Chim Acta* **2016**, *942*, pp. 121-138.
52. Zhang, S.; Lu, J.; Wang, S.; Mao, D.; Miao, S.; Ji, S. Multy-mycotoxins analysis in *Pheretima* using ultra-high-performance liquid chromatography tandem mass spectrometry based on a modified QuEChERS method. *J Chromatogr B* **2016**, *1035*, pp.31-41.
53. Dagnac, T.; Latorre, A.; Fernández, B.; Maria, M. Validation and application of a liquid chromatography-tandem mass spectrometry based method for the assessment of the cooccurrence of mycotoxins in maize silages from dairy farms in NW Spain. *Food Addit Contam: Part A* **2016**, *33(12)*, pp.1850-1863.
54. Sun, J.; Li, W.; Zhang, Y.; Hu, X.; Wu, L.; Wang, B. QuEChERS purification combined with ultrahigh-performance liquid chromatography tandem mass spectrometry for simultaneous quantification of 25 mycotoxins in cereals. *Toxins* **2016**, *8*, pp.375-392.
55. Smith, L.L.; Francis, K.A.; Johnson, J.T.; Gaskill, C.L. Quantification of fumonisin B1 and B2 in feed using FMOC pre-column derivatization with HPLC and fluorescence detection. *Food Chem* **2017**, *234*, pp.174-179.
56. Souto, P.C.M.C.; Jager, A.V.; Tonin, F.G.; Petta, T.; Di Gregório, M.C.; Cossalter, A-M.; Pinton, P.; Oswald, I.P.; Rottinghaus, G.E.; Oliveira, A.A.F. Determination of fumonisin B1 levels in body fluids and hair from piglets fed fumonisin B1-contaminates diets. *Food Chem Toxicol* **2017**, *108(A)*, pp.1-9.
57. Osteresch, B.; Viegas, S.; Cramer, B.; Humpf, H-U. Multi-mycotoxin analysis using dried blood spots and dried serum spots. *Anal BioanalChem* **2017**, *409*, pp.3369-3382.
58. Flores-Flores, M.E.; González-Peñas, E. An LC-MS/MS method for multi-mycotoxin quantification in cow milk. *Food Chem* **2017**, *218*, pp.378-385.
59. Zhao, Y.; Wan, L.; Bai, X.; Liu, Y.; Zhang, F.; Liu, Y.; Liao, X. Quantification of mycotoxins in vegetable oil by UPLC-MS/MS after magnetic solid-phase extraction. *Food Addit Contam: Part A* **2017**, *34(7)*,pp.1201-1210.
60. Annunziata, L.; Stramenga, A.; Visciano, P.; Schirone, M.; De Colli, L.; Novella, M.; Campana, G.; Scortichini, G. Simultaneous determination of aflatoxins, T-2 and HT-2 toxins, and fumonisins in cereal-derived products by QuEChERS extraction coupled with LC-MS/MS. *Anal BioanalChem* **2017**, *409*, pp.5143-5155.

61. Miró-Abella, E.; Herrero, P.; Canela, N.; Arola, L.; Borrull, F.; Ras, R.; Fontanals, N. Determination of mycotoxins in plant-based beverages using QuEChERS and liquid chromatography-tandem mass spectrometry. *Food Chem* **2017**, *229*, pp.366-372.
62. Abia, W.A.; Warth, B.; Ezekiel, C.N.; Sarkanj, B.; Turner, P.C.; Marko, D.; Krska, R.; Sulyok, M. Uncommon toxic microbial metabolite patterns in traditionally home-processed maize dish (fufu) consumed in rural Cameroon. *Food Chem Toxicol* **2017**, *107*, pp.10-19.
63. Hamed, A.M.; Arroyo-Manzanares, N.; García-Campaña, A.M.; Gámiz-Gracia, L. Determination of Fusarium toxins in functional vegetable milks applying salting-out-assisted liquid-liquid extraction combined with ultra-high performance liquid chromatography tandem mass spectrometry. *Food Addit Contam: Part A* **2017**, *34(11)*, pp.2033-2041.
64. Zhao, X.S.; Kong, W.J.; Wang, S.; Wei, J.H.; Yang, M.H. Simultaneous analysis of multiple mycotoxins in *Alpinia oxyphylla* by UPLC-MS/MS. *World Mycotoxin Journal* **2017**, *10(1), pp.41-51.*
65. Du, L.-J.; Chu, C.; Warner, E.; Wang, Q.-Y.; Hu, Y.-H.; Chai, K.-J.; Cao, J.; Peng, L.-Q.; Chen, Y.-B.; Yang, J.; Zhang, Q.-D. Rapid microwave-assisted dispersive micro-solid phase extraction of mycotoxins in food using zirconia nanoparticles. *J Chromatogr A* **2018**,*1561*, pp.1-12.
66. Huang, P.; Kong, W.; Wang, S.; Wang, R.; Lu, J.; Yang, M. Multiclass mycotoxins in lotus seeds analysed by an isotope-labelled internal standard-based UPLC-MS/MS. *J Pharm Pharmacol* **2018**, *70*, pp.1378-1388.
67. Zhang, B.; Chen, X.; Han, S.-Y.; Li, M.; Ma, T.-Z.; Sheng, W.-J.; Zhu, X. Simultaneous analysis of 20 mycotoxins in grapes and wines from Hexi corridor region (China): based on a QuEChERS–UHPLC–MS/MS method. *Molecules* **2018**, *23(8)*, 1926.
68. Abdallah, M.F.; Krska, R.; Sulyok, M. Occurrence of ochratoxins, fumonisin B2, aflatoxins(B1 and B2), and other secondary fungal metabolites in dried date palm fruits from Egypt: A mini-survey. *J Food Sci* **2018**, *83(2)*, pp.559-564.
69. De Baere, S.; Croubels, S.; Novak, B.; Bichl, G.; Antonissen, G. Development and validation of a UPLC-MS/MS and UPLC-HR-MS method for the determination of fumonisin B1 and its hydrolysed metabolites and fumonisin B2 in broiler chicken plasma. *Toxins* **2018**, *10(2), 62.*
70. Cladière, M.; Delaporte, G.; Le Roux, E.; Came, V. Multi-class analysis for simultaneous determination of pesticides, mycotoxins, process-induced toxicants and packaging contaminants in tea. *Food Chem* **2018**, *242*, pp.113-121.
71. Carballo, C.; Font, G.; Ferrer, E.; Berrada, H. Evaluation of mycotoxin residues on ready-to-eat food by chromatographic methods coupled to mass spectrometry in tandem. *Toxin* **2018**, *10(10)*, 243.
72. Park, J.; Kim, D.-H.; Moon, J.-Y.; An, J.-A.; Kim, Y.-W.; Chung, S.-H.; Lee, C. Distribution analysis of twelve mycotoxins in corn and corn-derived products by LC-MS/MS to evaluate the carry-over ratio during wet-milling. *Toxins* **2018**, *10(8)*, 319.
73. Šarkanj, B.; Ezekiel, C.N.; Turner, P.C.; Abia, W.A.; Rychlik, M.; Krska, R.; Sulyok, M.; Warth, B. Ultra-sensitive, stable isotope assisted quantification of multiple urinary mycotoxin exposure biomarkers. *Anal Chim Acta* **2018**, *1019*, pp.84-92.
74. González-Jartín, J. M; Alfonso, A.; Rodríguez, I.; Sainz, M. J.; Vieytes, M. R.; Botana, L. M. A. QuEChERS based extraction procedure coupled to UPLC-MS/MS detection for mycotoxins analysis in beer. *Food Chem* **2019**, *275*, pp.703-710.

75. Da Silva, L.P.; Madureira, F.; De Azevedo, E.; Ferreira, A.; Augusti, R. Development and validation of a multianalyte method for quantification of mycotoxins and pesticides in rice using a simple dilute and shoot procedure and UHPLC-MS/MS. *Food Chem* **2019**, *270*, pp.420-427.
76. Bessaire, T.; Perrin, I.; Tarres, A.; Bebius, A.; Reding, F.; Theurillat, V. Mycotoxins in green coffee: Occurrence and risk assessment. *Food Control* **2019**, *96*, pp.59-67.
77. Jedziniak, P.; Panasiuk, L.; Pietruszka, K.; Posyniak, A. Multiple mycotoxins analysis in animal feed with LC-MS/MS: Comparison of extract dilution and immune affinity clean-up. *J Sep Sci* **2019**, *42*, pp.1240-1247.
78. Nafuka, S. N.; Misihairabgwi, J. M.; Bock, R.; Ishola, A.; Sulyok, M.; Krska, R. Variation of fungal metabolites in sorghum malts used to prepare Namibian traditional fermented beverages Omalodu and Otombo. *Toxins* **2019**, *11(3)*, pp.165.
79. Abdallah, M. F.; Audenaert, K.; Lust, L.; Landschoot, S.; Bekaert, B.; Haesaert, G.; De Boevre, M.; De Saeger, S. Risk characterization and quantification of mycotoxins and their producing fungi in sugarcane juice: A neglected problem in a widely-consumed traditional beverage. *Food Control* **2020**, *108*, pp.106811.
80. Hort, V.; Nicolas, M.; Travel, A.; Jondreville, C.; Maleix, C.; Baéza, E.; Engel, E.; Guérin, T. Carry-over assessment of fumonisins and zearalenone to poultry tissues after exposure of chickens to a contaminated diet–A study implementing stable-isotope dilution assay and UHPLC-MS/MS. *Food Control* **2020**, *107*, pp.106789.
81. Thompson, V.S.; Maragos, C.M. Fiber-optic immunosensor for the detection of fumonisin B1. *J Agric Food Chem* **1996**, *44(4)*, pp.1041-1046.
82. Mullett, W.; Lai, E.P.C.; Yeung, J.M. Immunoassay of fumonisins by a surface plasmon resonance biosensor. *Anal Biochem* **1998**, 258(2), pp.161-167.
83. Ho, J.A.; Durst, R.A. Development of a flow-injection liposome immunoanalysis system for fumonisin B1. *Anal Chim Acta* **2000**, *414(1-2)*, pp.61-69.
84. Maragos, C.M.; Jolley, M.E.; Plattner, R.D.; Nasir, M.S. Fluorescence polarization as means for determination of fumonisin in maize. *Journal of Agricultural and Food Chem* **2011**, *49(2)*, pp.596-602.
85. Ligler, F.S.; Taitt, C.R.; Shriver-Lake, L.C.; Sapsford, K.E.; Shubin, Y.; Golden, J.P. Array biosensor for detection of toxins. *Anal BioanalChem* **2003**, *377(3)*, pp.469-477.
86. Quan, Y.; Zhang, Y.; Wang, S.; Lee, N.; Kennedy, I.R. A rapid and sensitive chemiluminescence enzyme-linked immunosorbent assay for the determinations of fumonisins B1 in food samples. *Anal Chim Acta* **2006**, *580(1)*, pp.1-8.
87. Lamberti, I.; Tanzarella, C.; Solinas, I.; Padula, C.; Mosiello, L. An antibody-based microarray assay for the simultaneous detection of aflatoxin B1 and fumonisin B1. *Mycotoxin Res* **2009**, *25*, pp.193-200.
88. Molinelli, A.; Grossalber, K.; Krska, R. A rapid lateral flow test for the determination of total type B fumonisins in maize. *Anal BioanalChem* **2009**, *395*, pp.1309-1316.
89. Anderson, G.P.; Kowtha, V.A.; Taitt, T.C. Detection of fumonisin B1 and Ochratoxin A in grain products using microsphere- based fluid array immunoassays. *Toxins* **2010**, *2(2)*, pp.297-309.
90. Kadir, M.K.; Tothill, I.E. Development of an electrochemical immunosensor for fumonisins detection in foods. *Toxins* **2010**, *2(4)*, pp.382-398.
91. Anfossi, L.; Calderara, M.; Baggiani, C.; Giovannoli, C.; Arletti, E.; Giraudi, G. Development and application of a quantitative lateral flow immunoassay for fumonisins in maize. *Anal Chim Acta* **2010**, *682(1-2)*, pp.104-109.

92. Wang, X.; Zhang, H.; Liu, H.; He, C.; Zhang, A.; Ma, J.; Ma, Y.; Wu, W. and Zheng, H. An immunoarray for the simultaneous detection of two mycotoxins, ochratoxin A and fumonisin B1. *J Food Saf* **2011**, *31(3)*, pp.408-416.
93. Mirasoli, M.; Buragina, A.; Dolci, L.S.; Simoni, P.; Anfossi, L.; Giraudi, G.; Roda, A. Chemiluminescence-based biosensor for fumonisins quantitative detection in maize samples. *Biosens Bioelectron* **2012**, *32(1)*, pp.283-287.
94. Li, Y.-S.; Zhou, Y.; Lu, S.-Y.; Guo, D.-J.; Ren, H.-L.; Meng, X.-M.; Zhi, B.-H.; Lin, C.; Wang, Z.; Li, X.-B.; Liu, Z.-S. Development of a one-step strip for rapid screening of fumonisins B_1, B_2 and B_3 in maize. *Food Control* **2012**, *24(1-2)*, pp.72-77.
95. Lattanzio, V.M.T.; Nirvarlet, N.; Lippolis, V.; Gatta, S.D.; Huet, A.-C.; Delahaut, P.; Granier, B.; Visconti, A. Multiplex dipstick immunoassay for semi-quantitative determination of *Fusarium* mycotoxins in cereals. *Anal Chim Acta* **2012**, *718*, pp.99-108.
96. Zou, L.; Xu, Y.; Li, Y.; He, Q.; Chen, B.; Wang, D. Development of a single-chain variable fragment antibody-based enzyme-linked immunosorbent assay for determination of fumonisin B1 in corn samples. *J Sci Food Agric* **2013**, *94(9)*, pp.1865-1871.
97. Peters, J.; Thomas, D.; Boers, E.; Rijk, T.; Berthiller, F.; Hasnoot, W.; Nielen, M.W.F. Colour-encoded paramagnetic microbead-based direct inhibition triplex flow cytometric immunoassay for ochratoxin A, fumonisins and zearalenone in cereals and cereal-based feed. *Anal BioanalChem* **2013**, *405(24)*, pp.7783-7794.
98. Wang, Y-K.; Yan, Y-X.; Ji, W-H.; Wang, H.; Li, S-Q.; Zou, Q.; Sun, J-H. Rapid simultaneous quantification of zearalenone and fumonisin B_1 in corn and wheat by lateral flow dual immunoassay. *J Agric Food Chem* **2013**, *61(21)*, pp.5031-5036.
99. Venkataramana, M.; Navya, K.; Chandranyaka, S.; Privanka, S.R.; Murali, H.S.; Batra, H.V. Development and validation of an immunochromatographic assay for rapid detection of fumonisin B1 from cereal samples. *J Food Sci Technol* **2014**, *51(9)*, pp.1920-1928.
100. Ezquerra, A.; Vidal, J.C.; Bonel, L.; Castillo, J.R. A validated multi-channel electrochemical immunoassay for rapid fumonisin B1 determination in cereal samples. *Anal Methods* **2015**, *7*, pp.3742-3749.
101. Masikini, M.; Mailu, S.N.; Tsegaye, A.; Njomo, N.; Molapo, K.M.; Ikpo, C.O.; Sunday, C.E.; Rassie, C.; Wilson, L.; Baker, P.G.L.; Iwuoha, E.I. A fumonisin immunosensor based on polyanilino-carbon nanotubes doped with palladium telluride quantum dots. *Sensors* **2015**, *15(1)*, pp.529-546.
102. Zangheri, M.; Nardo, F.; Anfossi, L.; Giovannoli, C.; Baggiani, C.; Roda, A.; Mirasoli, M. A multiplex chemiluminescent biosensor for type B-fumonisins and aflatoxin B1 quantitative detection in maize flour. *Analyst* **2015**, *140*, pp.358-365.
103. Yang, X.; Zhou, X.; Zhang, X.; Qing, Y.; Luo, M.; Liu, X.; Li, C.; Li, Y.; Xia, H.; Qiu, J. A highly sensitive electrochemical immunosensor for fumonisin B1 detection in corn using single-walled carbon nanotubes/chitosan. *Electroanalysis* **2015**, *27(11)*, pp.2679-2687.
104. Jodra, A.; López, M.A.; Escarpa, A. Disposable and reliable electrochemical magnetoimmunosensor for fumonisins simplified determinations in maize-based foodstuffs. *Biosens Bioelectron* **2015**, *64*, pp.633-638.
105. Shu, M.; Xu, Y.; Wang, D.; Liu, X.; Li, Y.; He, Q.; Tu, Z.; Qiu, Y.; Ji, Y.; Wang, X. Anti-idiotypic nanobody: A strategy for development of sensitive and green immunoassay for fumonisin B1. *Talanta* **2015**, *143*, pp.388-393.

106. Li, C.; Mi, T.; Conti, G.O.; Yu, Q.; Wen, K.; Shen, J.; Ferrante, M.; Wang, Z. Development of screening fluorescence polarization immunoassay for the simultaneous detections of fumonisins B1 and B2 in maize. *J Agric Food Chem* **2015**, *63(20)*, pp.4940-4946.
107. Ren, W.; Huang, Z.; Xu, Y.; Li, Y.; Ji, Y.; Su, B. Urchin-like gold nanoparticle-based immunochromatographic strip test for rapid detection of fumonisin B_1 in grains. *Anal BioanalChem* **2015**, *407(24)*, pp.7341-7348.
108. Lu, L.; Seenivasan, R.; Wang, Y.-C.; Yu, J.-H.; Gunasekaran, S. An electrochemical immunosensor for rapid sensitive detection of mycotoxins fumonisin B1 and deoxynivalenol. *Electrochim Acta* **2016**, *213*, pp.89-97.
109. Masikini, M.; Williams, A.R.; Sunday, C.E.; Waryo, T.T.; Nxusani, E.; Wilson, L.; Qakala, S. Bilibana, M.; Douman, S.; Jonnas, A.; Baker, P.G.L.; Iwuoha, E.I. Label free poly(2,5-dimethoxyaniline)-multi-walled carbon nanotubes impedimetric immunosensor for fumonisin B1 detection. *Materials* **2016**, *9(4)*, pp.273-286.
110. Di Nardo, F.; Baggiani, C.; Giovannoli, C.; Spano, G.; and Anfossi, L. Multicolor immunochromatographic strip test based on gold nanoparticles for the determination of aflatoxin B1 and fumonisins. *Microchim Acta* **2017**, *184(5)*, pp.1295-1304.
111. Urusov, A.E.; Petrakova, A.V.; Gubaydullina, M.K.; Zherdev, A. V.; Eremin, S. A.; Kong, D.; Liu, L.; Xu, C.; Dzantiev, B.B. High- sensitivity immunochromatographic assay for fumonisin B1 based on indirect antibody labelling. *Biotechnol Lett* **2017**, *39(5)*, pp.751-758.
112. Bánati, H.; Darvas, B.; Fehér-Tóth, S.; Czéh, A.; Székacs, A. Determination of mycotoxin production of Fusarium species in genetically modified maize varieties by quantitative flow immunocytometry. *Toxins* **2017**, *9(2)*, 70-81.
113. Tang, X.; Li, P.; Zhang, Z.; Zhang, Q.; Guo, J.; Zhang, W. An ultrasensitive gray-imaging- based quantitative immunochromatographic detection method for fumonisin B1 in agricultural products. *Food Control* **2017**, *80*, pp.333-340.
114. Peltomaa, R.; Benito-Peña, E.; Barderas, R.; Sauer, U.; González, M.; Moreno-Bondi, M.C. Microarray-based immunoassay with synthetic mimotopes for the detection of fumonisin B1. *Anal Chem* **2017**, *89*, pp.6216-6223.
115. Hao, K.; Suryoprabowo, S.; Hong, T.; Song, S.; Liu, L.; Zheng, Q.; Kuan, H. Immunochromatographic strip for ultrasensitive detection of fumonisin B1. *Food and Agr Immunol* **2018**, *29(1)*, pp.699-710.
116. Anfossi, L.; Di Nardo, F.; Cavalera, S.; Giovannoli, C.; Spano, G.; Speranskaya, E.S.; Goryacheva, I.Y.; Baggiani, C. A lateral flow immunoassay for straightforward determination of fumonisin mycotoxins based on the quenching of the fluorescence of CdSe/ZnS quantum dots by gold and silver nanoparticles. *Microchim Acta* **2018**, *185(2)*, 94.
117. Zhou,Y.; Huang. X.; Zhang, W.; Ji, Y.; Chen, R.; Xiong, Y. Multi-branched gold nanoflower-embedded iron porphyrin for colorimetric immunosensor. *Biosens Bioelectro* **2018**, *102*, pp.9-16.
118. Pagkali, V.; Petrou, P.S.; Makarona, E.; Peters, J.; Haasnoot, W.; Jobst, G.; Moser, I.; Gajos, K.; Budkowski, A.; Economou, A.; Misiakos, K.; Raptis, I.; Kakabakos, S.E. Simultaneous determination of aflatoxin B1, fumonisin B1 and deoxynivalenol in beer samples with a label-free monolithically integrated optoelectronic biosensor. *J Hazard Mater* **2018**, *359*, pp.445-453.
119. Peltomaa, R.; Amaro-Torres, F.; Carrasco, S.; Orellana, G.; Benito-Peña, E.; Moreno-Bondi, M.C. Homogeneous quenching immunoassay for fumonisin B1 based on gold nanoparticles and an epitope-mimicking yellow fluorescent protein. *ACS Nano* **2018**,*12*, pp.11333-11342.

120. Yu, S.; He, L.; Yu, F.; Liu, L.; Qu, C.; Qu, L.; Liu, J.; Wu, Y.; Wu, Y. A lateral flow assay for simultaneous detection of Deoxynivalenol, Fumonisin B1 and Aflatoxin B1. *Toxicon* **2018**, *156*, pp.23-27.
121. Lu, T.; Zhan, S.; Zhou, Y.; Chen, X.; Huang, X.; Leng, Y.; Xiong, Y.; Xu, Y. Fluorescence ELISA based on CAT-regulated fluorescence quenching of CdTe QDs for sensitive detection of FB1. *Anal Methods* **2018**, *10***,** pp.5797-5802.
122. Jie, M.; Yu, S.; Yu, F.; Liu, L.; He, L.; Li, Y.; Zhang, H.; Ou, L.; Harrington, P.; Wu, Y. An ultrasensitive chemiluminescence immunoassay for fumonisin B1 detections in cereals based on gold-coated magnetic nanoparticles. *J Sci Food Agric* **2018**, *98(9)*, pp.3384-3390.
123. Li, Z.; Sheng, W.; Li, S.; Shi, Y.; Zhang, Y.; Wang, S. Development of a gold nanoparticle enhanced enzyme linked immunosorbent assay based on monoclonal antibodies for the detections of fumonisin B1, B2 and B3 in maize. *Anal Methods* **2018**, *10*, pp.3506-3513.
124. Chen, X.; Liang, Y.; Zhang, W.; Leng, Y.; Xiong, Y. A colorimetric immunoassay based on glucose oxidase-induced AuNP aggregation for the detection of fumonisin B1. *Talanta* **2018**, *186*, pp.29-35.
125. Sheng, W.; Wu, H.; Ji, W.; Li, Z.; Chu, F.; Wang, S. Visual non-instrumental on-site detection of fumonisin B1, B2, and B3 in cereal samples using a clean-up combined with gel-based immunoaffinity test column assay. *Toxins* **2018**, *10(4)*, pp.165-179.
126. Wang, X.; Park, S.-G.; Ko, J.; Xiao, X.; Giannini, V.; Maier, S.A.; Kim, D.-H.; Choo, J. Sensitive and reproducible immunoassay of multiple mycotoxins using surface-enhanced Raman scattering mapping on 3D plasmonic nanopillar arrays. *Small* **2018**, *14*, pp.1801623.
127. Zhang, X.; Wang, Z.; Fang, Y.; Sun, R.; Cao, T.; Paudyal, N.; Fang, W.; Song, H. Antibody microarray immunoassay for simultaneous quantification of multiple mycotoxins in corn samples. *Toxins* **2018**, *10(10)*, pp.415.
128. Shu, M.; Xu, Y.; Dong, J.; Zhong, C.; Hammock, B.D.; Wang, W.; Wu, G. Development of a noncompetitive idiometric nanobodies phage immumoassay for the determination of fumonisin B1. *Food Agr Immunol* **2019**, *30(1)*, pp.510-521.
129. Lu, L.; Gunasekaran, S. Dual-channel ITO-microfluidic electrochemical immunosensor for simultaneous detection of two mycotoxins. *Talanta* **2019**, *194*, pp.709-716.
130. Qu, J.; Xie, H.; Zhang, S.; Luo, P.; Guo, P.; Chen, X.; Ke, Y.; Zhuang, J.; Zhou, F.; Jiang, W. Multiplex flow cytometric immunoassays for high-throughput screening of multiple mycotoxin residues in milk. *Food Anal Methods* **2019**, *12*, pp. 877-886.
131. Duan, H.; Li, Y.; Shao, Y.; Huang, X.; Xiong, Y. Multicolor quantum dot nanobeads for simultaneous multiplex immunochromatographic detection of mycotoxins in maize. *Sens Actuators, B. Chemical* **2019**, *291, pp. 411-417.*
132. Cheng, Z. X.; Ang, W. L.; Bonanni, A. Electroactive Nanocarbon Can Simultaneously Work as Platform and Signal Generator for Label-Free Immunosensing*. ChemElectroChem* **2019***, 6(14)*, pp. 3615-3620.
133. Zhan, S.; Zheng, L.; Zhou, Y.; Wu, K.; Duan, H.; Huang, X.; Xiong, Y. A Gold Growth-Based Plasmonic ELISA for the Sensitive Detection of Fumonisin B1 in Maize. Toxins **2019**, *11(6)*, pp. 323.
134. Shao, Y.; Duan, H.; Zhou, S.; Ma, T.; Guo, L.; Huang, X.; Xiong, Y. Biotin–Streptavidin System-Mediated Ratiometric Multiplex Immunochromatographic Assay for Simultaneous and Accurate Quantification of Three Mycotoxins. J Agric Food Chem **2019**, *67(32)*, pp. 9022-9031.
135. Huang, X.; Huang, T.; Li, X.; Huang, Z. Flower-like gold nanoparticles-based immunochromatographic test strip for rapid simultaneous detection of fumonisin B1 and deoxynivalenol in Chinese traditional medicine. J Pharm Biomed Anal **2020**, *177*, pp. 112895.

136. Hou, S.; Ma, J.; Cheng, Y.; Wang, H.; Sun, J.; Yan, Y. One-stop rapid detection of fumonisin B1, dexyonivalenol and zearalenone in grains. *Food Control* **2020**, pp.107107.
137. Yang, H.; Zhang, Q.; Liu, X.; Yang, Y.; Yang, Y.; Liu, M.; Li, P.; Zhou, Y. Antibody-biotin-streptavidin-horseradish peroxidase (HRP) sensor for rapid and ultra-sensitive detection of fumonisins. *Food Chem* **2020**, *316*, pp.126356.
138. Ren, W.; Xu, Y.; Huang, Z.; Li, Y.; Tu, Z.; Zou, L.; He, Q.; Fu, J.; Liu, S.; Hammock, B. D. Single-chain variable fragment antibody-based immunochromatographic strip for rapid detection of fumonisin B1 in maize samples. *Food Chem* **2020**, pp. 126546.
139. Liu, Z.; Hua, Q.; Wang, J.; Liang, Z.; Li, J.; Wu, J.; Shen, X.; Lei, H.; Li, X. A smartphone-based dual detection mode device integrated with two lateral flow immunoassays for multiplex mycotoxins in cereals. Biosens Bioelectron **2020,** pp.112178.
140. Lee, K.M.; Herrman, T. Determination and prediction of fumonisin contamination in Maize by surface-enhanced Raman spectroscopy (SERS). *Food Bioprocess Technol* **2016**, *9(4)*, pp.588-603.
141. Smolinska-Kempisty, K.; Guerreiro, A.; Canfarotta, F.; Cáceres, C.; Whitcombe, M.J.; Piletsky, S. A comparison of the performance of molecularly imprinted polymer nanoparticles for small molecule targets and antibodies in the ELISA format. Sci Rep **2016**, *6*, pp. 37638.
142. Zhang, W.; Xiong, H.; Chen, M.; Zhang, X.; Wang, S. Surface-enhanced molecularly imprinted electrochemiluminescence sensor based on Ru@SiO2 for ultrasensitive detection of fumonisin B1. *Biosens Bioelectron* **2017**, *96*, pp. 55-61.
143. Munawar, H.; Smolinska-Kempisty, K.; Cruz, A.G.; Canfarotta, F.; Piletska, E.; Karim, K.; Piletsky, S.A. Molecular imprinted polymer nanoparticle-based assay (MINA): application for fumonisin B1 determination. *Analyst* **2018**,*143*, pp.3481-3488.
144. Mao. L.; Ji, K.; Yao, L.; Xue, X.; Wen, W.; Zhang, X.; Wang, S. Molecularly imprinted photoelectrochemical sensor for fumonisin B1 based on GO-CdS heterojunction. *Biosens Bioelectron* **2019**, **127**, pp. 57-63.
145. Munawar, H.; Safaryan, A. H.; De Girolamo, A.; Garcia-Cruz, A.; Marote, P.; Karim, K.; Lippolis, V.; Pascale, M.; Piletsky, S. A. Determination of Fumonisin B1 in maize using molecularly imprinted polymer nanoparticles-based assay. *Food Chem* **2019**, *298*, 125044.
146. Chotchuang, T.; Cheewasedtham, W.; Jayeoye, T. J.; Rujiralai, T. Colorimetric determination of fumonisin B1 based on the aggregation of cysteamine-functionalized gold nanoparticles induced by a product of its hydrolysis. *Microchim Acta* **2019**, *186(9)*, pp.655.
147. Li, L.; Chen, W.; Li, H.; Iqbal, J.; Zhu, Y.; Wu, T.; Du, Y. Rapid determination of fumonisin (FB1) by syringe SPE coupled with solid-phase fluorescence spectrometry. *SAA* **2020**, *226*, pp.117549.
148. McKeague, M.; Bradley, C.R.; De Girolamo, A.; Visconti, A.; Miller, J.D.; DeRosa, M.C. Screening and initial binding assessment of fumonisin B1 aptamers. Int J Mol Sci **2010**, *11(12)*, pp.4864-4881.
149. Chen, X.; Huang, Y.; Duan, N.; Wu, S.; Xia, Y.; Ma, X.; Zhu, C.; Jiang, Y.; Ding, Z.; Wang, Z. Selection and characterization of single stranded DNA aptamers recognizing fumonisin B1. *Microchim Acta* **2014**, *181*, pp.1317-1324.
150. Frost, N.R.; McKeague, M.; Falcioni, D.; DeRosa, M.C. An in solution assay for interrogation of affinity and rational minimer design for small molecules binding aptamers. *Analyst* **2015**, *140*, pp.6643-6651.
151. Wu, S.; Duan, N.; Ma, X.; Xia, Y.; Wang, H.; Wang, Z.; Zhang, Q. Multiplexed fluorescence resonance energy transfer aptasensor between upconversion nanoparticles and graphene oxide for the simultaneous determination of mycotoxins. *Anal Chem* **2012**, *84(14)*, pp.6263-6270.

152. Wu, S.; Duan, N.; Li X.; Tan, G.; Ma, X.; Xia, Y.; Wang, Z.; Wang, H. Homogenous detection of fumonisin B_1 with a molecular beacon based on fluorescence energy transfer between $NaYF_4$:YB, Ho upconversion nanoparticles and gold nanoparticles. *Talanta* **2013**, *116(15)*, pp.611-618.
153. Wang, W.F.; Wu, S.; Ma, X.Y.; Xia, Y.; Wang, Z.P. Novel methods for fumonisin B1 detection based on AuNPs labelling and aptamer recognition. *J Food Sci Biotech* **2013**, *32(5)*, pp.501-508.
154. Yue, S.; Jie, X.; Wei, L.; Bin, C.; Dou, W.D.; Yi, Y., QingXia, L.; JianLin, L.; TieSong, Z. Simultaneous detection of ochratoxin A and fumonisin B1 in cereal samples using an aptamer-photonic crystal encoded suspension array. *Anal Chem* **2014**, *86(23)*, pp.11797-11802.
155. Zhao, Y.; Luo, Y.; Li, T.; Song, Q. AuNPs driven electrochemiluminescence aptasensors for sensitive detection of fumonisin B1. *RSC Advances* **2014**, *4*, pp.57709-57714.
156. Chen, X.; Huang, Y.; Ma, X.; Jia, F.; Guo, X.; Wang, Z. Impedimetric aptamer-based determination of the mold toxin fumonisin B_1. *Microchim Acta* **2015**, *182(9-10)*, pp.1709-1714.
157. Chen, X.; Bai, X.; Li, H.; Zhang, B. Aptamer-based microcantilever array biosensor for detection of fumonisin B_1. *RSC Advances* **2015**, *5*, pp.35448-35452.
158. Shi, Z.-Y.; Zheng Y.-T.; Zhang, H.-B.; He, C.-H.; Wu, W.-D.; Zhang, H.-B. DNA electrochemical aptasensor for detecting fumonisin B1 based on graphene and thionine nanocomposite. *Electroanalysis* **2015**, *27(5)*, pp.1097-1103.
159. Gui, H.; Jin, Q.; Zhang, Y.; Wang, X.; Yang, Y.; Shao, C.; Cheng, C.; Wei, F.; Yang, Y.; Yang, M.; Song, H. Development of an aptamer/ fluorescence dye PicoGreen-based method for detection of fumonisin B1. *Sheng Wu Gong Cheng Xue Bao* **2015**, *31(9)*, pp.1393–1400.
160. Ren, C.; Li, H.; Lu, X.; Quian, J.; Zhu, M.; Chen, W.; Liu, Q.; Hao, N; Li, H.; Wang, K. A disposable aptasensing device for label-free detection of fumonisin B1 by integrating PDMS film-based micro-cell and screen-printed carbon electrode. *Sens Actuators, B* **2017**, *251*, pp.192-199.
161. Yang, Y.; Li, W.; Shen, P.; Liu, R.; Li, Y.; Xu, J.; Zheng, Q.; Zhang, Y.; Li, J.; Zheng. T. Aptamer fluorescence signal recovery screening for multiplex mycotoxins in cereal samples based on photonic crystal microsphere suspension array. *Sens Actuators, B* **2017**, *248*, pp.351.358.
162. Wang, C.; Qian, J.; An, K.; Huang, X.; Zhao, L.; Liu, Q.; Hao, N.; Wang, K. Magneto-controlled aptasensor for simultaneous electrochemical detection of dual mycotoxins in maize using metal sulfide quantum dots coated silica as labels. *Biosens Bioelectron* **2017**, *89*, pp.802-809.
163. Molinero-Fernández, A.; Moreno-Guzmán, M.; Ángel López, M.; Escarpa, A. Biosensing strategy for simultaneous and accurate quantitative analysis of mycotoxins in food samples using unmodified graphene micromotors. *Anal Chem* **2017**, *89*, pp.10850-10857.
164. Tian, H.; Sofer, Z.; Pumera, M.; Bonanni, A. Investigation on the ability of heteroatom-doped graphen for biorecognition. *Nanoscale* **2017**, 9, pp.3530-3536.
165. 王红旗, 王俊艳, 洪慧杰, 尹海燕, Maragos, C., 张 玲, 刘继红.伏马毒素 B1 核酸适配体链置换探针的筛选及应用. *农产品质量与安全* **2017**,*1*, pp.44-48.
166. Liu, R.; Li, W.; Cai, T.; Deng, Y.; Ding, Z.; Liu, Y.; Zhu, X.; Wang, X.; Liu, J.; Liang, B.; Zheng, T.; LI, J. TiO_2 nanolayer-enhanced fluorescence for simultaneous multiplex mycotoxin detection by aptamer microarrays on a porous silicon surface. ACS *Appl Mater Interfaces* **2018**, *10*, pp.14447-14453.
167. Cheng, Z.; Bonanni, A. All-in-One: Electroactive nanocarbon as simultaneous platform and label for single-step biosensing. *Nanomaterials* **2018**, *24*, pp.6380-6385.

168. Molinero-Fernández, A.; Jodra, A.; Moreno-Guzmán, M.; López, M.A.; Escarpa, A. Magnetic reduced graphene oxide/nickel/platinum nanoparticles micromotors for mycotoxin analysis. *Chem Eur J* **2018**, *24*, pp.7172-7176.
169. Hao, N.; Lu, J.; Zhou, Z.; Hua, R.; Wang, K. A pH-resolved colorimetric biosensor for simultaneous multiple target detection. *ACS Sensors* **2018**, *3*, pp.2159-2165.
170. Niazi, S.; Khan, I.M.; Yan, L.; Khan, M.I.; Mohsin, A.; Duan, N.; Wu, S.; Wang, Z. Simultaneous detection of fumonisin B1 and ochratoxin A using dual-color, time-resolved luminescent nanoparticles ($NaYF_4$: Ce, Tb and NH_2-Eu/DPA@SiO_2) as labels. *Anal BioanalChem* **2019**; *411*, pp.1453-1465.
171. Wang, C.; Huang, X.; Tian, X.; Zhang, X.; Yu, S.; Chang, X.; Ren, Y.; Qian, J. A multiplexed FRET aptasensor for the simultaneous detection of mycotoxins with magnetically controlled graphene oxide/Fe3O4 as a single energy acceptor. *Analyst* **2019**, *144(20)*, 6004-6010.
172. Wei, M.; Zhao, F.; Feng, S.; Jin, H. A novel electrochemical aptasensor for fumonisin B 1 determination using DNA and exonuclease-I as signal amplification strategy. *BMC Chemistry* **2019**, *13(1)*, pp.1-6.
173. Han, Z.; Tang, Z.; Jiang, K.; Huang, Q.; Meng, J.; Nie, D.; Zhao, Z. Dual-target electrochemical aptasensor based on co-reduced molybdenum disulfide and Au NPs (rMoS2-Au) for multiplex detection of mycotoxins. *Biosens Bioelectron* **2020**, *150*, pp.11894.
174. Wei, M.; Xin, L.; Feng, S.; Liu, Y. Simultaneous electrochemical determination of ochratoxin A and fumonisin B1 with an aptasensor based on the use of a Y-shaped DNA structure on gold nanorods. *Microchim Acta* **2020**, *187(2)*, pp.1-7.
175. He, D.; Wu, Z.; Cui, B.; Xu, E. Aptamer and gold nanorod–based fumonisin B1 assay using both fluorometry and SERS. *Microchim Acta* **2020**, *187(4)*, pp.1-8.
176. Tao, Z.; Zhou, Y.; Li, X.; Wang, Z. Competitive HRP-Linked Colorimetric Aptasensor for the Detection of Fumonisin B1 in Food based on Dual Biotin-Streptavidin Interaction. *Biosensors* **2020**, *10(4)*, pp.31.
177. He, D.; Wu, Z.; Cui, B.; Jin, Z.; Xu, E. A fluorometric method for aptamer-based simultaneous determination of two kinds of the fusarium mycotoxins zearalenone and fumonisin B1 making use of gold nanorods and upconversion nanoparticles. *Microchim Acta* **2020**, 187, pp.254.
178. Kesici, E.; Erdem, A. Impedimetric detection of Fumonisin B1 and its biointeraction with fsDNA. *Int J Biol Macromol* **2019**, *139*, pp.
179. Siler, D.J.; Gilchrist, D.G. Determination of host-selective phytotoxins from *Alternaria alternata* f.sp. *lycopersici* as their maleyl derivatives by high-performance liquid chromatography. *J Chromatogr* **1982**, *238*, pp.167-173.
180. Sydenham, E.W.; Gelderblom, W.C.A.; Thiel, P.G.; Marasas, W.F.O. Evidence for the natural occurrence of fumonisin B1, a mycotoxin produced by *Fusarium moniliforme,* in corn. *J Agric Food Chem* **1990**, *38(1)*, pp.285-290.
181. Shepard, G.S.; Sydenham, E.W.; Thiel, P.G.; Gelderblom, C.A. Quantitative determination of fumonisins B1 and B2 by high-performance liquid chromatography with fluorescence detection. *J Liq Chromatogr* **1990**, *13(10)*, pp.2077-2087.
182. Bordin, K.; Rosim, R.E.; Neeff, D.V.; Rottinghaus, G.E.; Oliveira, C.A.F. Assessment of dietary intake of fumonisin B1 in São Paulo, Brazil. *Food Chem* **2014**, *155*, pp.174-178.
183. Holcomb, M.; Thompson, H.C.; Hankins, L.J. Analysis of fumonisin B1 in rodent feed by gradient elution HPLC using precolumn derivatization with FMOC and fluorescence detection. *J Agric Food Chem* **1993**, *41(5)*, pp.764-767.

184. Food Standards Agency. 2019. Incidents annual reports 2006-2017. Available online: https://www.food.gov.uk/about-us/reports-and-accounts (Accessed on 10 April 2020).
185. Gilbert-Sandoval, I.; Wesseling, S.; Rietjens, I.M. Occurrence and probabilistic risk assessment of fumonisin B1, fumonisin B2 and deoxynivalenol in nixtamalized maize in Mexico City. *Toxins* **2020**, *12(10)*, p.644.
186. Yapo, A.E.; Strub, C.; Durand, N.; Ahoua, A.R.C.; Schorr-Galindo, S.; Bonfoh, B.; Fontana, A.; Koussémon, M. Mass spectrometry-based detection and risk assessment of mycotoxin contamination of 'kankankan'used for roasted meat consumption in Abidjan, Côte d'Ivoire. *Food Addit Contam: Part A* **2020**, *37(9)*, pp.1564-1578.
187. Sulyok, M.; Krska, R.; Senyuva, H. Profiles of fungal metabolites including regulated mycotoxins in individual dried Turkish figs by LC-MS/MS. *Mycotoxin Res* **2020**, *36(4)*, pp.381-387.
188. Zhang, L.; Sun, Y.; Liang, X.; Yang, Y.; Meng, X.; Zhang, Q.; Li, P.; Zhou, Y. Cysteamine triggered "turn-on" fluorescence sensor for total detection of fumonisin B1, B2 and B3. *Food Chem* **2020**, *327*, pp.127058.
189. Hou, S.; Ma, J.; Cheng, Y.; Wang, H.; Sun, J.; Yan, Y. Quantum dot nanobead-based fluorescent immunochromatographic assay for simultaneous quantitative detection of fumonisin B1, dexyonivalenol, and zearalenone in grains. *Food Control* **2020**, *117*, pp.107331.
190. Guo, L.; Wang, Z.; Xu, X.; Xu, L.; Kuang, H.; Xiao, J.; Xu, C. Europium nanosphere-based fluorescence strip sensor for ultrasensitive and quantitative determination of fumonisin B 1. *Anal Methods* **2020**, *12*, pp.5229-5235.
191. Munawar, H.; Garcia-Cruz, A.; Majewska, M.; Karim, K.; Kutner, W.; Piletsky, S.A., Electrochemical determination of fumonisin B1 using a chemosensor with a recognition unit comprising molecularly imprinted polymer nanoparticles. *Sens Actuators, B* **2020**, *321*, pp.128552.
192. Hines, H.B.; Brueggemann, E.E.; Holcomb, M.; Holder, C.L. Fumonisin B1 analysis with capillary electrophoresis–electrospray ionization mass spectrometry. *Rapid Commun Mass Spectrom* **1995**, *9(6)*, pp.519-524.
193. Holcomb, M., Thompson Jr, H.C. Analysis of fumonisin B1 in corn by capillary electrophoresis with fluorescence detection of the FMOC derivative. *J Microcolumn Sep* **1995**, *7(5)*, pp.451-454.
194. Maragos, C.M. Capillary zone electrophoresis and HPLC for the analysis of fluorescein isothiocyanate-labeled fumonisin B1. Journal of Agricultural and *Food Chem* **1995**, *43(2)*, pp.390-394.
195. Maragos, C.M. Detection of the mycotoxin fumonisin B1 by a combination of immunofluorescence and capillary electrophoresis. *Food and Agr Immunol* **1997**, *9(3)*, pp.147-157.
196. Kecskeméti, Á.; Nagy, C.; Biró, P.; Szabó, Z.; Pócsi, I.; Bartók, T.; Gáspár, A. Analysis of fumonisin mycotoxins with capillary electrophoresis–mass spectrometry. *Food Addit Contam: Part A* **2020**, *37(9)*, pp.1553-1563.
197. Jiang, D.; Huang, C.; Shao, L.; Wang, X.; Jiao, Y.; Li, W.; Chen, J.; Xu, X. Magneto-controlled aptasensor for simultaneous detection of ochratoxin A and fumonisin B1 using inductively coupled plasma mass spectrometry with multiple metal nanoparticles as element labels. *Anal Chim Acta* **2020**, *1127*, pp.182-189.
198. Wu, Z.; He, D.; Cui, B.; Jin, Z.; Xu, E.; Yuan, C.; Liu, P.; Fang, Y.; Chai, Q. Trimer-based aptasensor for simultaneous determination of multiple mycotoxins using SERS and fluorimetry. *Microchim Acta* **2020**, *187(9)*, pp.1-7.

199. Zheng, Y.T.; Zhao, B.S.; Zhang, H.B.; Jia, H.; Wu, M. Colorimetric aptasensor for fumonisin B1 detection by regulating the amount of bubbles in closed bipolar platform. *J Electroanal Chem* **2020**, *877*, p.114584.
200. Mirón-Mérida, V.A.; González-Espinosa, Y.; Gong, Y.Y.; Guo, Y.; Goycoolea, F.M. Comparison of the Performances of Two Aptamers on a Colorimetric Assay for the Quantification of Fumonisin B1. *MDPI Proceedings* **2020**, *60(1)*, pp.19.